

000 001 002 003 004 005 006 007 008 009 010 011 012 013 014 015 016 017 018 019 020 021 022 023 024 025 026 027 028 029 030 031 032 033 034 035 036 037 038 039 040 041 042 043 044 045 046 047 048 049 050 051 052 053 FEEDBACK DESCENT: OPEN-ENDED TEXT OPTIMIZATION VIA PAIRWISE COMPARISON

Anonymous authors

Paper under double-blind review

ABSTRACT

Current preference learning methods discard the rich explanations humans naturally provide when comparing examples, collapsing detailed feedback into binary signals. We introduce *Feedback Descent*, a framework that widens this information bottleneck by leveraging textual feedback to enable directed optimization in text space rather than weight space. We show that in-context learning can transform structured feedback into gradient-like directional information, enabling targeted edits of text artifacts such as prompts, code, and JSON. Unlike prior approaches that collapse judgments into single bits, our evaluators pair each comparison with textual feedback, which functions as high-bandwidth supervision. The iteration loop is done purely at inference time, without modifying any model weights, and is task-agnostic. We evaluate Feedback Descent on three diverse domains and find that it outperforms state-of-the-art prompt optimization (GEPA), reinforcement learning methods (GRPO, REINVENT), and even specialized graph-based molecular optimizers. In the DOCKSTRING molecule discovery benchmark, Feedback Descent identifies novel drug-like molecules surpassing the 99.9th percentile of a database with more than 200,000 compounds across six protein targets.

1 INTRODUCTION

A central goal of machine learning is building systems that can perform tasks that are difficult or impossible even for humans. Reinforcement learning is a powerful framework that accomplishes this goal, since it can optimize with respect to feedback on its own outputs, rather than relying on supervised examples of desired outputs. Indeed, recent language models have demonstrated impressive feats in domains like math and programming (OpenAI, 2024; DeepSeek-AI et al., 2025; Google DeepMind, 2025; Zhu et al., 2024) through a combination of reinforcement learning and text-based reasoning. Unfortunately, existing reinforcement learning frameworks are designed to learn from impoverished supervision signals, typically either scalar rewards or pairwise preference data, where each annotation conveys at most a single bit per pair. These bottlenecks discard information about *why* one behavior is better and *how* to improve—information available in environment feedback or easily elicited from humans during annotation.

Our goal is to widen this information bottleneck, i.e., significantly increase the information the system can extract per unit of experience (Silver & Sutton, 2025). Collecting more detailed feedback is straightforward, e.g., with brief rationales explaining preferences; the challenge is turning such feedback into measurable improvement. Because free-form feedback does not define a differentiable objective, it cannot directly drive weight updates via backpropagation. Our core idea is to use an *optimization loop in text space* rather than weight space: we leverage the in-context learning capabilities of language models to translate feedback into targeted edits of text artifacts (e.g., code, prompts, molecules, JSON configs, etc) that improve a final performance objective.

To that end, we introduce *Feedback Descent*, a framework for continual optimization in text space. At each iteration, we generate a new candidate artifact based on all previous feedback. We compare this candidate against the current best artifact, and the evaluator returns a preference along with textual feedback explaining the choice. If the candidate is preferred, it becomes the new best. Repeating this loop yields semantically local, feedback-aligned improvements that implement gradient-like steps in text space. See Fig. 1 for a conceptual illustration. We provide theoretical intuition for why Feedback Descent can be effective. Under appropriate assumptions about feedback quality

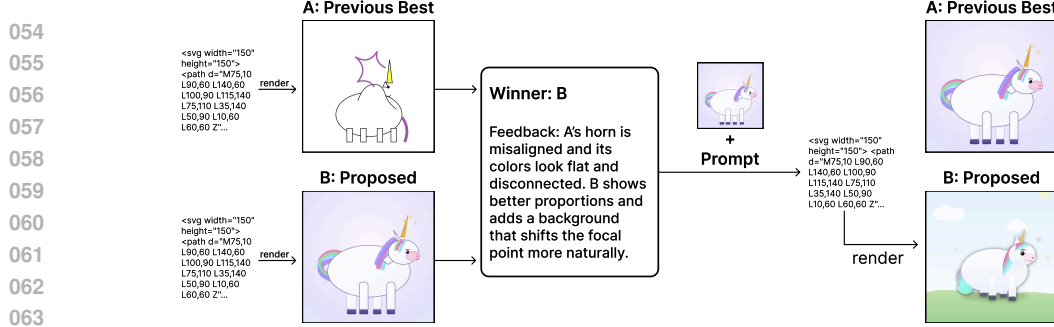


Figure 1: A conceptual illustration of feedback descent. At each iteration, we compare the previous best artifact with a new candidate. The evaluator provides both a pairwise preference and textual feedback. Preferences ensure the selection of better candidates, while feedback accumulates directional information that guides semantically meaningful edits.

and problem structure, we demonstrate that textual feedback can provide directional information, enabling efficient optimization.

Our contributions are threefold. First, we introduce *Feedback Descent*, an inference-time optimization framework that uses pairwise preferences with textual rationales to provide directional updates entirely in text space. Second, we demonstrate its generality across three domains: (i) SVG design, where iterative feedback produces judge-aligned visual improvements beyond direct prompting under both scratch and rubric-aware initializations; (ii) prompt optimization on IFBench, where Feedback Descent surpasses GEPA on Qwen3-8B and remains competitive with the strongest methods on GPT-4.1 Mini; and (iii) molecule discovery on DOCKSTRING, where Feedback Descent outperforms reinforcement learning approaches such as REINVENT and rivals specialized graph-based algorithms. Third, we show that the novel molecules discovered by Feedback Descent exceed not only the 99.9th percentile of a 260,000-compound database but, on several targets, surpass the best molecule present in the dataset.

2 FEEDBACK DESCENT: OPEN-ENDED TEXT OPTIMIZATION

We propose Feedback Descent, a framework for open-ended optimization of text-native artifacts whose quality is easier to *judge* than to *construct*. Feedback Descent converts comparative textual feedback into directed semantic edits and iterates in a self-improvement loop. As a running example, consider optimizing SVG code to render better images of a unicorn. Current vision-language models can reliably compare two renderings and explain the choice, even if writing high-quality SVG from scratch is difficult. Through Feedback Descent, we can convert these explanations into directed edits that aim to produce an artifact that is better than all previous ones.

2.1 PROBLEM SETUP

Let \mathcal{S} be the space of token sequences, and let $x \in \mathcal{S}$ denote an artifact (e.g., SVG code). Given a current incumbent $x_t^* \in \mathcal{S}$ and a candidate $x \in \mathcal{S}$, the evaluator returns

$$E(x, x_t^*) \rightarrow (p \in \{0, 1\}, r \in \mathcal{S}), \quad (1)$$

where $p = 1$ indicates $x \succ x_t^*$ and r is a textual feedback explaining *why* the winner is better and *how* to improve. We append r_t to a history $\mathcal{R}_t = \{(x_1, r_1), \dots, (x_t, r_t)\}$ and iterate, keeping track of the current best artifact x_t^* .

2.2 FEEDBACK DESCENT

Feedback Descent operates as an iterative optimization loop that maintains a single best artifact x_t^* and progressively improves it through feedback-guided mutations and comparative evaluation. Throughout, we use \mathcal{M} to denote the language model used for generating improved candidates.

Initialization and termination. We initialize x_0^* by prompting a language model with the task description alone (e.g., "Generate SVG code for a unicorn"), providing a reasonable starting point

108 without prior feedback. The algorithm runs for a fixed budget of T iterations or until convergence
 109 (defined as no improvement for k consecutive iterations).

110 **Proposing semantic mutations via prompting.** The mutation step leverages a language model’s
 111 in-context learning capabilities. Given the current best artifact x_t^* and accumulated feedback
 112 r_1, r_2, \dots, r_{t-1} , we prompt the model to generate improved candidates:

$$x_t = \mathcal{M}(\text{“Improve } x_t^* \text{ using feedback: } \mathcal{R}_{t-1}\text{”}) \quad (2)$$

113 These prompts are intentionally minimal: the optimization signal comes
 114 from the accumulated feedback rather than heavy prompt engineering.
 115 They include basic task context, the current
 116 best artifact, and feedback from previous com-
 117 parisons. Complete prompt templates for each
 118 domain are provided in [Section C.3](#).

119 **Selection and update.** We compare the new
 120 candidate x_t against the current best x_t^* using
 121 the evaluator $E(x_t, x_t^*)$, which returns both a
 122 binary preference p_t and a textual feedback
 123 r_t . In our running SVG example, examples
 124 of feedback include “adjust the stroke width”,
 125 “make sure the legs are connected to the body”,
 126 and “add a shadow to the unicorn’s mane”. Re-
 127 gardless of the preference outcome, we always
 128 add the feedback to our history: $\mathcal{R}_{t+1} = \mathcal{R}_t \cup \{(x_t, r_t)\}$. If $p_t = 1$ (candidate is preferred), we
 129 update $x_{t+1}^* = x_t$; otherwise we keep $x_{t+1}^* = x_t^*$. We summarize the overall process in [Algorithm 1](#).

132 2.3 ANALOGY TO GRADIENT DESCENT

133 The key algorithmic insight is best understood by analogy to gradient descent. Just as gradients
 134 provide the direction of steepest ascent under local linearity, textual feedback can suggest plausible
 135 directions of improvement in semantic space. For our SVG example, if the feedback indicates “needs
 136 more defined horn shape,” we expect that a small edit to the horn shape that preserves overall structure
 137 will likely be an improvement.

138 Of course, textual feedback is not a literal gradient. It is approximate and occasionally contradictory—
 139 optimization with such feedback does not have convergence guarantees in the same way that gradient
 140 descent does. Instead, feedback acts as a heuristic directional cue, offering higher-bandwidth
 141 supervision than a binary preference signal or a scalar reward, just as first-order optimization is
 142 fundamentally faster than zeroth-order optimization (Nemirovski & Yudin, 1983; Agarwal et al.,
 143 2012; Nesterov & Spokoiny, 2017). We hypothesize that an open-ended optimization loop based on
 144 such cues can succeed, supported by prior evidence that language models reliably translate textual
 145 instructions into concrete modifications. Examples include generating code changes (Chen et al.,
 146 2021; Austin et al., 2021; Nijkamp et al., 2022; Wang et al., 2023b; Roziere et al., 2023; Guo
 147 et al., 2024; Lozhkov et al., 2024; CodeGemma Team et al., 2024), following complex multi-step
 148 instructions (Ouyang et al., 2022; Wei et al., 2022a; Chung et al., 2022; Longpre et al., 2023; Zhang
 149 et al., 2024), targeted text modifications (Schick et al., 2022; Du et al., 2022; Madaan et al., 2023;
 150 Welleck et al., 2023; Kim et al., 2023), and decomposing high-level goals into executable action
 151 sequences (Schick et al., 2023; Parisi et al., 2022; Yao et al., 2023b; Qin et al., 2023; Wang et al.,
 152 2023a; Agarwal et al., 2025).

153 **Why directional information helps.** Zeroth-order methods that rely only on function evaluations
 154 or binary preferences suffer severe dimension-dependent slowdowns: convergence rates degrade
 155 exponentially as the search space grows (Nemirovski & Yudin, 1983; Nesterov & Spokoiny, 2017).
 156 In contrast, first-order methods exploit gradient information to achieve dimension-free convergence
 157 under standard assumptions. Textual feedback provides an approximation to such directional in-
 158 formation. Even when individual rationales are imperfect, their aggregate message across failures
 159 continually refines the direction of improvement. We formalize this intuition in [Section A](#), showing
 160 that under idealized assumptions, rationale-guided updates can achieve linear convergence rates inde-
 161 pendent of effective dimensionality, while zeroth-order baselines scale exponentially worse. These
 162 results provide motivation rather than rigorous guarantees for the discrete text domains we study

162 empirically. In Section 4, we show that Feedback Descent indeed produces consistent improvements
 163 across tasks, validating that such heuristic directional cues are sufficient to drive open-ended text
 164 optimization.

166 3 RELATED WORK

168 **Preference Learning.** Preference learning methods learn from pairwise comparisons (Christiano
 169 et al., 2017; Ouyang et al., 2022; Azar et al., 2023; Ethayarajh et al., 2024; Munos et al., 2024);
 170 recent advances include bypassing the need for a reward model (Rafailov et al., 2023), iterative
 171 optimization under KL constraints (Xiong et al., 2023), and adaptive scaling techniques (Wang et al.,
 172 2024). However, these methods fundamentally compress complex human reasoning into binary or
 173 scalar preferences, foregoing the rich explanatory content that humans can naturally provide alongside
 174 judgments (Wirth et al., 2017). Unlike prior work that relies solely on scalar feedback despite the
 175 complexity of human judgment, we leverage detailed textual rationales to widen this information
 176 bottleneck, allowing for more efficient adaptation.

177 **Evolutionary Algorithms and Gradient-Free Optimization.** Feedback Descent can be viewed as
 178 an evolutionary algorithm (Golberg, 1989; Holland, 1992), in which candidates are iteratively mutated
 179 and accepted based on fitness. While the black-box nature of modern LLMs has spurred interest
 180 in applying gradient-free approaches (Guo et al., 2023; Sun et al., 2022; Chen et al., 2024; Lange
 181 et al., 2024), these methods face fundamental challenges in high-dimensional spaces. More broadly,
 182 zeroth-order methods (Chen et al., 2019) face convergence rates that scale poorly with dimension,
 183 which is consistent with our experimental results comparing with reinforcement learning methods
 184 in Section 4. Feedback Descent explores whether textual rationales can provide useful directional
 185 information for optimization, similar to how Nie et al. (2024) shows that LLMs can be effective
 186 optimizers when provided with directional feedback from historical traces. Our contribution is in
 187 operationalizing an effective *directed mutation operator* via accumulated textual feedback.

188 **Optimizing Compound AI Systems.** Compound AI systems, i.e., modular architectures involving
 189 multiple LLM invocations and complex control flow, such as agents or scaffolding techniques (Yao
 190 et al., 2023b), present unique optimization challenges due to their modularity. Several approaches have
 191 emerged to tackle this complexity, including optimization for searching and bootstrapping few-shot
 192 in-context examples (Khattab et al., 2022; 2024; Opsahl-Ong et al., 2024), backpropagating textual
 193 feedback between components (Yuksekgonul et al., 2024), and reflective prompt evolution (Agrawal
 194 et al., 2025). However, these methods focus on optimizing individual components or connections
 195 within fixed architectures. In contrast, Feedback Descent provides a general-purpose text optimization
 196 framework that treats LLMs as optimizers for any text-representable artifact. While compound AI
 197 systems are one promising application domain, our approach generalizes beyond AI systems to
 198 optimize standalone text artifacts such as SVG code and molecular representations.

199 **Inference-Time Optimization for LLMs.** Inference-time optimization improves performance with-
 200 out weight updates by performing additional computation at generation. This paradigm includes self-
 201 critique and refinement cycles (constitution-guided critique (Bai et al., 2022); Self-Refine (Madaan
 202 et al., 2023)) test-time scaling via best-of- N , multi-step reasoning, and tree search (Cobbe et al., 2021;
 203 Zelikman et al., 2022; Yao et al., 2023a), and iterative prompt optimization (Zhou et al., 2022; Yang
 204 et al., 2023; Pryzant et al., 2023). Several works report that strategically allocating inference-time
 205 compute yields large gains (Snell et al., 2024; Brown et al., 2025; Geiping et al., 2025; Zhou et al.,
 206 2025). We build on the growing consensus that natural language is a particularly powerful medium
 207 for inference-time improvement. Natural language traces enable models to reason effectively in
 208 complex environments (Lampinen et al., 2022; Wei et al., 2022b), and language models can reliably
 209 map textual instructions to concrete modifications (Chen et al., 2021; Austin et al., 2021; Saunders
 210 et al., 2022; Scheurer et al., 2023). However, existing methods often rely on random sampling of
 211 self-generated critiques, which may be noisy or fail to capture external preferences. In contrast, we
 212 leverage external rationales as directional information, enabling guided search in the semantic space.

213 4 EXPERIMENTS

214 We evaluate Feedback Descent across three diverse domains—visual design, prompt optimization,
 215 and molecule discovery—to demonstrate its generality and effectiveness. Through our experiments,

Model	Condition	Anatomy	Cyber	Geom	Min.	Retro	Story
GPT-4o-mini	Scratch	95.2 \pm 8.3	97.6 \pm 4.1	87.7 \pm 5.3	100.0 \pm 0.0	100.0 \pm 0.0	100.0 \pm 0.0
	Informed	92.1 \pm 9.3	91.2 \pm 4.8	93.0 \pm 7.8	92.8 \pm 7.7	69.8 \pm 47.2	95.6 \pm 3.8
GPT-5-mini	Scratch	100.0 \pm 0.0					
	Informed	92.1 \pm 9.3	89.9 \pm 7.0	96.3 \pm 3.2	95.9 \pm 3.6	96.1 \pm 3.4	100.0 \pm 0.0

Table 1: **Win rates after five iterations comparing Feedback Descent against direct prompting under two conditions: from *Scratch* and *Informed* of the judge rubric.** We show means and standard deviations across 3 random seeds. **Iterative feedback consistently improves SVG designs over direct prompting.**

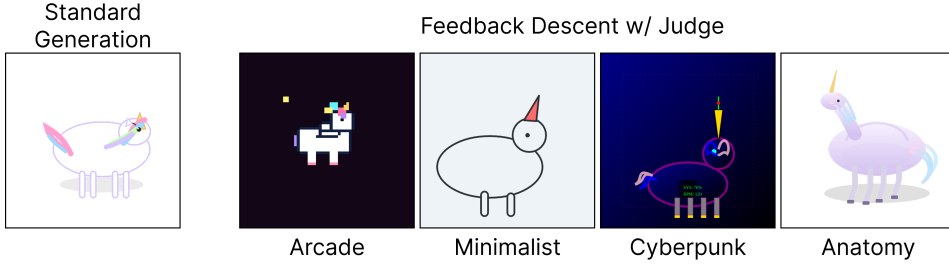


Figure 2: Example unicorn images generated by Feedback Descent under four different judge criteria: retro arcade, minimalist, cyberpunk, and anatomy. **Feedback Descent yields visually distinct unicorns aligned with the aesthetic criteria preferred by each judge.**

we aim to answer the following questions. First, we ask whether Feedback Descent exhibits generality by working robustly across qualitatively different domains. Second, we test sample efficiency, evaluating whether iterative, rationale-guided feedback enables higher-quality solutions with fewer model queries than existing optimizers. Third, we measure outcome quality, assessing whether Feedback Descent can produce artifacts (SVGs, prompts, and molecules) that not only satisfy rubrics and constraints but also surpass state-of-the-art methods on established benchmarks.

4.1 EXPERIMENTAL DOMAINS

We describe each evaluation domain and how we obtain pairwise comparisons augmented with textual rationales.

SVG optimization. Taking inspiration from Bubeck et al. (2023), we ask models to output SVG code for illustrations of unicorns. We use a set of six diverse judge prompts, each preferring a different aesthetic: accurate *anatomy*, *cyberpunk* futurism, *geometric* abstraction, *minimalist*, *retro arcade* pixel-art motifs, and *storybook* illustrations. We compare rendered SVGs using GPT-5-mini, which outputs both a binary preference and short textual feedback. To mitigate order bias, we perform two judgments with swapped image orders (A-B and B-A) and declare a winner only if both judgments are consistent. Otherwise, we try again, up to three times, and discard if no consistent winner emerges.

Prompt optimization. We follow the setup of GEPA (Agrawal et al., 2025) on IFFBench (Pyatkin et al., 2025), a benchmark for evaluating precise constraint-following (e.g., “answer only with yes or no”). We design a two-stage system that first produces an answer and then rewrites it to satisfy constraints, and we jointly optimize the prompts for both stages using Feedback Descent. Optimization is driven by the 150 training examples: candidate prompts are updated based on performance on the training set and textual feedback describing which constraints were satisfied or violated. All candidate prompts are scored on the 300 validation examples, and the prompt with the highest validation accuracy rate is selected. We report performance on a test set of 294 held-out examples.

Molecule discovery. We evaluate on molecular docking tasks using DOCKSTRING (García-Ortegón et al., 2022) docking scores and drug-likeness (QED). DOCKSTRING provides a realistic drug discovery setting where molecules are evaluated based on their predicted binding affinity to medically relevant targets rather than simple physicochemical properties. We focus on challenging optimization tasks across six protein targets: ADRB1, PGR, PPARA, PPARG, CDK2, and F2. Following DOCKSTRING, we compute the combined score $s = -\text{Vina} - 10 \times (1 - \text{QED})$. We

Method	Qwen3-8B	GPT-4.1 Mini
DSPy Default (Khattab et al., 2024)	36.90	47.79
MIPROv2 (Opsahl-Ong et al., 2024)	36.22	49.15
GRPO (Shao et al., 2024)	35.88	—
GEPA (Agrawal et al., 2025)	38.61	52.72
GEPA+Merge (Agrawal et al., 2025)	28.23	55.95
Ours	44.22 ± 3.15	54.59 ± 2.46

Table 2: Comparison of prompt optimization methods on IFBench. We report scores for Qwen3-8B and GPT-4.1 Mini under matched rollout budgets. **Feedback Descent outperforms all baselines on Qwen3-8B, and is competitive with the state-of-the-art for GPT-4.1 Mini.**

represent molecules as SMILES strings (Weininger, 1988) and evaluate using DOCKSTRING’s molecular docking pipeline to compute Vina scores (binding affinity). The feedback system provides rich structured information, including RDKit molecular descriptors (Landrum, 2006), similarity searches against known compounds from molecular databases (Liu et al., 2007; Gilson et al., 2016; Gaulton et al., 2012; Mendez et al., 2019), and detailed docking results. In the system prompt, we also provide the LLM information about the protein target obtained from the UniProt database (The UniProt Consortium, 2023). Together, this provides the LLM with detailed feedback on molecular properties that affect binding affinity, drug-likeness violations, and comparisons to known active compounds.

4.2 SVG OPTIMIZATION

We evaluate iterative feedback against direct prompting across two generators, GPT-4o-mini and GPT-5-mini. The direct prompting baseline receives the full evaluation rubric and is tasked with producing a single best design. Feedback Descent instead begins with an initial set of candidates, and through 5 rounds of structured feedback and improvement, refines designs using judge comparisons that reflect aesthetic criteria. We test two initialization regimes: **Scratch**, which starts from images simply instructed to generate images of unicorns, and **Informed**, which starts from the strongest direct generations conditioned on the rubric, determined by the LLM judge.

Results. Table 1 shows the win rates after 5 iterations. For both GPT-4o-mini and GPT-5-mini, Feedback Descent reliably improves outputs over the initial population. Furthermore, qualitative examples in Fig. 2 demonstrate that the procedure consistently produces unicorns whose visual style diverges across judges, aligning with aesthetic criteria such as geometry, minimalism, or retro arcade motifs.

Iterative feedback can elicit better outputs from the same model

Because of a generator–verifier gap, even prompting with the exact judge rubric is suboptimal for SVG generation. Feedback Descent elicits better images from the same generator by iteratively proposing improvements guided by feedback.

4.3 PROMPT OPTIMIZATION

We compare Feedback Descent against five baselines: the default prompt implemented in the DSPy program (Khattab et al., 2024, Default), a Bayesian optimization approach for selecting instructions and demonstrations (Opsahl-Ong et al., 2024, MIPROv2), online reinforcement learning (Shao et al., 2024, GRPO), and a reflective prompt evolution method (Agrawal et al., 2025, GEPA). All baselines are run under matched rollout budgets for fair comparison, and the reported baseline results are from Agrawal et al. (2025).

Each example produces pointwise feedback about which constraints were satisfied or violated. To construct the pairwise feedback for Feedback Descent, we stratify the examples into quadrants based on whether each prompt resulted in a correct response. We then ask the model to propose textual descriptions of inputs where these discrepancies arise. We then statistically validate each hypothesis, filtering for ones that correspond to consistent differences in performance between the prompts. This process distills the true global differences between the two prompts.

	Method	ADRB1	PGR	PPARA	PPARG	CDK2	F2
DOCKSTRING (N=260155)	Top 50%	5.305	3.478	4.549	4.210	4.385	4.168
	Top 90%	8.785	7.878	7.987	7.658	7.733	7.477
	Top 99%	9.620	8.703	8.718	8.449	8.453	8.139
	Top 99.9%	10.209	9.260	9.230	9.012	8.979	8.722
	Top 99.99%	<u>10.742</u>	<u>9.723</u>	9.821	9.518	9.509	9.252
	Best Molecule	<u>11.330</u>	<u>9.742</u>	9.907	9.529	9.534	<u>9.311</u>
	GP-BO [†] (Tripp et al., 2021)	10.552	9.307	9.680	9.485	9.067	8.686
	Graph MCTS [†] (Jensen, 2019)	8.883	7.819	7.363	7.134	7.777	6.310
	Graph GA [†] (Jensen, 2019)	9.145	8.670	8.598	8.327	8.288	8.102
	SMILES GA (Brown et al., 2019)	9.334	8.335	9.052	8.560	8.268	7.984
	REINVENT (Olivecrona et al., 2017)	9.018	8.267	8.430	8.347	8.226	8.139
	TextGrad (Yuksekgonul et al., 2024)	8.531	8.057	7.953	7.256	8.174	7.357
	Feedback Descent	10.623	9.615	9.919	10.187	9.803	9.300

Table 3: Comparison of molecule optimization methods on six protein targets. Fragment-based algorithms (denoted by [†]) operate directly on molecular graphs, giving them structural priors unavailable to purely text-based methods. For each target, the top generative result is in **bold**, and any population in the DOCKSTRING that exceeds the best generative result is underlined. **Feedback Descent rivals or surpasses specialized molecular optimizers across all six targets.**

Table 2 shows that Feedback Descent achieves the highest score on Qwen3-8B (44.22 vs. 38.61 for GEPA) and remains competitive with GEPA and GEPA+Merge on GPT-4.1 Mini (54.59 vs. 55.95). These results indicate that structured, iterative feedback drives steady improvements in prompt optimization, even though other optimizers such as GEPA exploit problem structure.

Grounded Summaries Enable Reliable Prompt Optimization

By summarizing a large set of pointwise rationales into a global comparison between two prompts, Feedback Descent yields more reliable prompts.

4.4 MOLECULE OPTIMIZATION (DOCKSTRING)

We compare against baselines implemented in the mol_opt repository (Gao et al., 2022). Our comparisons include a genetic algorithm (Brown et al., 2019, SMILES GA), reinforcement learning (Olivecrona et al., 2017, REINVENT), fragment-based algorithms (Jensen, 2019, Graph MCTS/GA), and Bayesian optimization on molecular graphs (Tripp et al., 2021, GP-BO). Because fragment-based methods exploit graph-level structural priors, the most direct comparison is to the text-only baselines: SMILES-GA and REINVENT. Nonetheless, we report results against all methods to provide a complete picture of performance. **Results.** Table 3 summarizes optimization outcomes across six protein targets. For each target, we benchmark Feedback Descent against specialized molecular optimization algorithms as well as ligands from the DOCKSTRING dataset, which comprises both decoy and experimentally active ligands. Feedback Descent is competitive with all baselines and achieves the strongest scores on several targets (e.g., ADRB1, PGR, PPARG, CDK2, F2). On multiple proteins, it matches or exceeds the 99.9th and even 99.99th percentiles of the DOCKSTRING database, including surpassing the best molecule present in the dataset itself ($N = 260155$). These findings show that Feedback Descent, a purely text-based method, can rival or outperform specialized graph-based algorithms, despite lacking handcrafted structural priors. Fig. 4 shows optimization trajectories for PPARG. Feedback Descent achieves competitive trajectories relative to specialized methods, often reaching high-scoring regions of chemical space with comparable or fewer oracle calls. This pattern holds across targets, suggesting that the method generalizes rather than relying on idiosyncrasies of a single protein system.

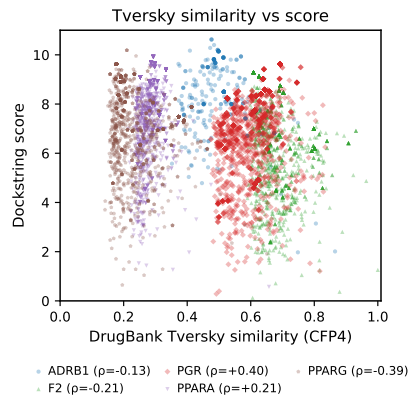


Figure 3: Scatter plots of Tversky similarity to approved drugs against docking scores, showing weak or negative correlations across targets. **High-scoring molecules discovered by Feedback Descent are far from any known drugs.**

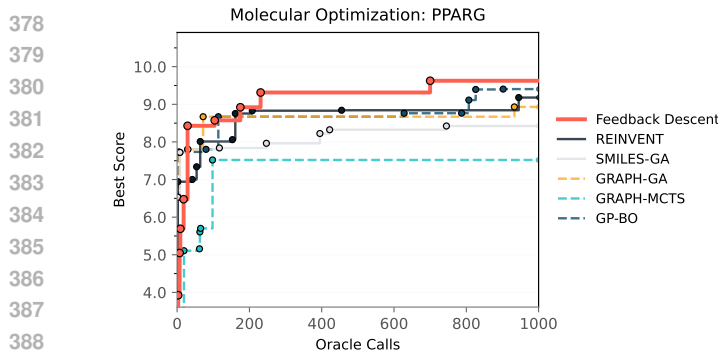


Figure 4: Optimization trajectories on PPARG showing docking scores over oracle calls for Feedback Descent and specialized baselines. **Feedback Descent quickly improves molecular docking scores within the first few hundred oracle calls.**

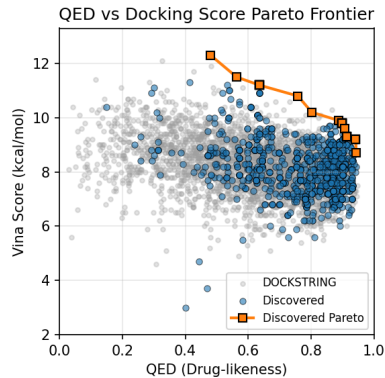


Figure 5: Pareto frontier of docking affinity vs. drug-likeness, comparing Feedback Descent molecules (blue) to the DOCKSTRING dataset (gray). **Feedback Descent finds novel molecules that meet or surpass known ones.**

Analysis of discovered molecules. Fig. 5 illustrates the Pareto frontier between docking affinity (Vina score) and drug-likeness (QED) for PPARG. Feedback Descent recovers molecules that sit on or above the DOCKSTRING frontier, indicating that improvements in affinity are not achieved at the expense of reduced drug-likeness. See Fig. 6 in the appendix for the full set of Pareto frontiers across all targets. These results show that feedback-guided search yields candidates that are not only potent but also balanced along multiple drug-relevant dimensions.

We also examine novelty by plotting Tversky similarity (CFP4 fingerprints) to approved DrugBank molecules against docking scores in Fig. 3. Across all targets, the correlations are weak or negative (Spearman ρ between -0.39 and 0.40), showing that high-scoring candidates discovered by Feedback Descent do not simply recycle functional groups from existing drugs but instead explore novel regions of chemical space. For CDK2, no comparison is shown: the target lacks any fully approved drugs in DrugBank with orthosteric binding as part of their mechanism of action, and thus does not satisfy our filtering criteria for inclusion.

Feedback Descent Can Discover Novel Targeted Molecules

Feedback Descent, operating in a purely textual form, consistently identifies novel molecules that surpass high-percentile baselines in DOCKSTRING. This demonstrates that iterative, feedback-guided optimization can enable models to genuinely explore unknown design spaces beyond their training distribution.

5 DISCUSSION

This paper presents Feedback Descent, an inference-time framework that improves text artifacts through structured pairwise feedback. We validate it on visual design, prompt optimization, and molecule discovery, showing that text can serve as an optimizable medium, not just static data. Unlike parameter tuning, this approach can leverage richer textual signals, allowing for continual improvement without requiring retraining.

Limitations. The method relies on strong evaluators, which may be scarce in some domains. Training models to produce reliable feedback remains a prerequisite for harder tasks. For creative domains, strictly “following the gradient” may be limiting; balancing refinement with exploration is an important next step.

432 ETHICS STATEMENT
433

434 This work adheres to the ICLR Code of Ethics. Our research focuses on improving preference
435 learning methods through textual rationales, which have positive implications for AI alignment
436 and human-AI collaboration. The methods developed could potentially be misused to optimize for
437 harmful content; the same risk exists with any preference learning approach. Our contribution lies in
438 making such optimization more efficient rather than enabling fundamentally new capabilities.

439 REPRODUCIBILITY STATEMENT
440

441 We are committed to ensuring the reproducibility of our results. Complete experimental details,
442 including hyperparameters and evaluation protocols, are provided in the main text and appendix. All
443 datasets used in our experiments are either publicly available or will be released upon publication. The
444 proofs are presented with full detail in [Section A](#) with all assumptions clearly stated. Implementation
445 details for Feedback Descent, including prompting strategies and in-context learning procedures, are
446 documented in the appendix.

447
448 REFERENCES
449

450 Alekh Agarwal, Peter L Bartlett, Pradeep Ravikumar, and Martin J Wainwright. Information-theoretic
451 lower bounds on the oracle complexity of stochastic convex optimization. *IEEE Transactions on*
452 *Information Theory*, 58(5):3235–3249, 2012.

453 Mayank Agarwal, Ibrahim Abdelaziz, Kinjal Basu, Merve Unuvar, Luis A Lastras, Yara Rizk, and
454 Pavan Kapanipathi. Toolrm: Outcome reward models for tool-calling large language models. *arXiv*
455 *preprint arXiv:2509.11963*, 2025.

456 Lakshya A Agrawal, Shangyin Tan, Dilara Soylu, Noah Ziems, Rishi Khare, Krista Opsahl-Ong,
457 Arnav Singhvi, Herumb Shandilya, Michael J Ryan, Meng Jiang, et al. Gepa: Reflective prompt
458 evolution can outperform reinforcement learning. *arXiv preprint arXiv:2507.19457*, 2025.

459 Jacob Austin, Augustus Odena, Maxwell I. Nye, Maarten Bosma, Henryk Michalewski, David Dohan,
460 Ellen Jiang, Carrie J. Cai, Michael Terry, Quoc V. Le, and Charles Sutton. Program synthesis with
461 large language models. *arXiv preprint arXiv:2108.07732*, 2021.

462 Mohammad Gheshlaghi Azar, Mark Rowland, Bilal Piot, Daniel Guo, Daniele Calandriello, Michal
463 Valko, and Remi Munos. A general theoretical paradigm to understand learning from human
464 preferences. *arXiv preprint arXiv:2310.12036*, 2023.

465 Yuntao Bai, Saurav Kadavath, Sandipan Kundu, Amanda Askell, Jackson Kernion, Andy Jones, Anna
466 Chen, Anna Goldie, Azalia Mirhoseini, Cameron McKinnon, et al. Constitutional ai: Harmlessness
467 from ai feedback. *arXiv preprint arXiv:2212.08073*, 2022.

468 Nathan Brown, Marco Fiscato, Marwin HS Segler, and Alain C Vaucher. Guacamol: Benchmarking
469 models for de novo molecular design. *Journal of Chemical Information and Modeling*, 59(3):
470 1096–1108, 2019. doi: 10.1021/acs.jcim.8b00839.

471 Tom B. Brown et al. s1: Simple test-time scaling. *arXiv preprint arXiv:2501.19393*, 2025.

472 Sébastien Bubeck, Varun Chandrasekaran, Ronen Eldan, Johannes Gehrke, Eric Horvitz, Ece Kamar,
473 Peter Lee, Yin Tat Lee, Yuanzhi Li, Scott Lundberg, et al. Sparks of artificial general intelligence:
474 Early experiments with gpt-4. *arXiv preprint arXiv:2303.12712*, 2023.

475 Mark Chen, Jerry Tworek, Heewoo Jun, Qiming Yuan, Henrique Ponde de Oliveira Pinto, Jared Ka-
476 plan, Harri Edwards, Yura Burda, Nicholas Joseph, Greg Brockman, Alex Ray, Raul Puigdomenech,
477 Alec Radford, Vedant Sastry, Ilya Sutskever, Daniel M. Ziegler, Amanda Dennison, Marius Ervin,
478 William Perez, Sallaheddine Karaa, Sarah Kluska, Jerome Lespiau, Tom B. Brown, and David Wu.
479 Evaluating large language models trained on code. *arXiv preprint arXiv:2107.03374*, 2021.

480 Xiangyi Chen, Sijia Liu, Kaidi Xu, Xingguo Li, Xue Lin, Mingyi Hong, and David Cox. Zo-adamm:
481 Zeroth-order adaptive momentum method for black-box optimization. 2019.

486 Xiangyi Chen, Sijia Liu, and Mingyi Hong. Derivative-free optimization for low-rank adaptation in
 487 large language models. *arXiv preprint arXiv:2403.01754*, 2024.

488

489 Paul F Christiano, Jan Leike, Tom Brown, Miljan Martic, Shane Legg, and Dario Amodei. Deep
 490 reinforcement learning from human preferences. *Advances in Neural Information Processing
 491 Systems*, 30, 2017.

492

493 Hyung Won Chung, Le Hou, Shayne Longpre, Barret Zoph, Yi Tay, William Fedus, Eric Li, Xuezhe
 494 Wang, Mostafa Dehghani, Siddhartha Brahma, Albert Webson, Shixiang Shane Gu, Zhuyun Dai,
 495 Mirac Suzgun, Xinyun Chen, Aakanksha Chowdhery, Sharan Narang, Gaurav Mishra, Adams Yu,
 496 Vincent Zhao, Yanping Huang, Andrew Dai, Hongkun Yu, Slav Petrov, Ed H. Chi, Jeff Dean, Jacob
 497 Devlin, Adam Roberts, Denny Zhou, Quoc V. Le, and Jason Wei. Scaling instruction-finetuned
 498 language models. *arXiv preprint arXiv:2210.11416*, 2022.

499

500 Karl Cobbe, Vineet Kosaraju, Mohammad Bavarian, Mark Chen, Heewoo Jun, Lukasz Kaiser,
 501 Matthias Plappert, Jerry Tworek, Jacob Hilton, Reiichiro Nakano, Christopher Hesse, and John
 502 Schulman. Training verifiers to solve math word problems. *arXiv preprint arXiv:2110.14168*,
 503 2021.

504

505 CodeGemma Team, Heri Zhao, et al. Codegemma: Open code models based on gemma. *arXiv
 506 preprint arXiv:2406.11409*, 2024.

507

508 DeepSeek-AI, Daya Guo, Dejian Yang, Haowei Zhang, Junxiao Song, Ruoyu Zhang, Runxin Xu,
 509 Qihao Zhu, Shirong Ma, Peiyi Wang, et al. Deepseek-r1: Incentivizing reasoning capability
 510 in llms via reinforcement learning. *arXiv preprint arXiv:2501.12948*, 2025. URL <https://arxiv.org/abs/2501.12948>.

511

512 Wanyu Du, Vipul Raheja, Dhruv Kumar, Zae Myung Kim, Melissa Lopez, and Dongyeop Kang. Read,
 513 revise, repeat: A system demonstration for human-in-the-loop iterative text revision. *In2Writing*,
 514 2022.

515

516 Kawin Ethayarajh, Winnie Xu, Niklas Muennighoff, Dan Jurafsky, and Douwe Kiela. Kto: Model
 517 alignment as prospect theoretic optimization. *arXiv preprint arXiv:2402.01306*, 2024.

518

519 Wenhao Gao, Tianfan Fu, Jimeng Sun, and Connor W Coley. Sample efficiency matters: A benchmark
 520 for practical molecular optimization. *arXiv preprint arXiv:2206.12411*, 2022.

521

522 Miguel García-Ortegón, Gregor N. C. Simm, Austin J. Tripp, José Miguel Hernández-Lobato,
 523 Matthias R. Bauer, and Sergio Bacallado. Dockstring: Easy molecular docking yields better
 524 benchmarks for ligand design. *Journal of Chemical Information and Modeling*, 62(15):3486–3502,
 525 2022. doi: 10.1021/acs.jcim.1c01334.

526

527 Anna Gaulton, Louisa J Bellis, A Patricia Bento, Jon Chambers, Mark Davies, Anne Hersey, Yvonne
 528 Light, Shaun McGlinchey, David Michalovich, Bissan Al-Lazikani, and John P Overington.
 529 Chemb3d: a large-scale bioactivity database for drug discovery. *Nucleic Acids Research*, 40(D1):
 530 D1100–D1107, 2012. doi: 10.1093/nar/gkr777.

531

532 Jonas Geiping, Sean McLeish, Neel Jain, John Kirchenbauer, Siddharth Singh, Brian R Bartoldson,
 533 Bhavya Kailkhura, Abhinav Bhatele, and Tom Goldstein. Scaling up test-time compute with latent
 534 reasoning: A recurrent depth approach. *arXiv preprint arXiv:2502.05171*, 2025.

535

536 Michael K Gilson, Tiqing Liu, Michael Baitaluk, George Nicola, Linda Hwang, and Justin Chong.
 537 Bindingdb in 2015: a public database for medicinal chemistry, computational chemistry and
 538 systems pharmacology. *Nucleic Acids Research*, 44(D1):D1045–D1053, 2016. doi: 10.1093/nar/
 539 gkv1072.

540

541 David E Goldberg. Genetic algorithms in search, optimization, and machine learning. *Addison Wesley*,
 542 1989(102):36, 1989.

543

544 Google DeepMind. Gold-medalist performance in solving olympiad geometry with alphageometry2.
 545 *arXiv preprint arXiv:2502.03544*, 2025. URL <https://arxiv.org/abs/2502.03544>.

540 Daya Guo, Shuo Ren, Shuai Lu, Zhangyin Feng, Duyu Tang, Shijie Liu, Long Zhou, Nan Duan,
 541 Alexey Svyatkovskiy, Shengyu Fu, et al. Deepseek-coder: When the large language model meets
 542 programming – the rise of code intelligence. *arXiv preprint arXiv:2401.14196*, 2024.

543

544 Zerui Guo, Tianxiang Sun, Xipeng Qiu, and Xuanjing Huang. When gradient descent meets derivative-
 545 free optimization: A match made in black-box scenario. *arXiv preprint arXiv:2305.10013*, 2023.

546

547 John H Holland. *Adaptation in natural and artificial systems: an introductory analysis with applica-
 548 tions to biology, control, and artificial intelligence*. MIT press, 1992.

549

550 Jan H Jensen. A graph-based genetic algorithm and generative model/monte carlo tree search for
 551 the exploration of chemical space. *Chemical Science*, 10(12):3567–3572, 2019. doi: 10.1039/
 552 C8SC05372C.

553

554 Omar Khattab, Christopher Potts, and Matei Zaharia. Demonstrate-search-predict: Composing
 555 retrieval and language models for knowledge-intensive nlp. *arXiv preprint arXiv:2212.14024*,
 556 2022.

557

558 Omar Khattab, Arnav Singhvi, Paridhi Maheshwari, Zhiyuan Zhang, Keshav Santhanam, Sri Vard-
 559 hamanan, Saiful Haq, Ashutosh Sharma, Thomas T Joshi, Hanna Moazam, Heather Miller, Matei
 560 Zaharia, and Christopher Potts. Dspy: Compiling declarative language model calls into self-
 561 improving pipelines. *arXiv preprint arXiv:2310.03714*, 2024.

562

563 Seonghyeon Kim, Sukmin Cho, Doyoung Kim, Sejin Kim, Chacha Chen, Ekaterina Kochmar,
 564 Hwajung Hong, and Alice Oh. Help me think: A simple prompting strategy for non-experts to
 565 create customized content with models. *arXiv preprint arXiv:2208.08232*, 2023.

566

567 Andrew K Lampinen, Nicholas Roy, Ishita Dasgupta, Stephanie Cy Chan, Allison Tam, James
 568 McClelland, Chen Yan, Adam Santoro, Neil C Rabinowitz, Jane Wang, and Felix Hill. Tell me
 569 why! Explanations support learning relational and causal structure. In *Proceedings of the 39th
 570 International Conference on Machine Learning*, volume 162 of *Proceedings of Machine Learning
 571 Research*, pp. 11868–11890. PMLR, 2022.

572

573 Greg Landrum. Rdkit: Open-source cheminformatics, 2006. URL <http://www.rdkit.org>.

574

575 Robert Tjarko Lange, Yingtao Tian, and Yujin Tang. Large language model-based evolutionary
 576 optimizer: Reasoning with elitism. *arXiv preprint arXiv:2403.02054*, 2024.

577

578 Tiqing Liu, Yuhmei Lin, Xin Wen, Robert N Jorissen, and Michael K Gilson. Bindingdb: a web-
 579 accessible database of experimentally determined protein–ligand binding affinities. *Nucleic Acids
 580 Research*, 35(suppl_1):D198–D201, 2007. doi: 10.1093/nar/gkl999.

581

582 Shayne Longpre, Le Hou, Tu Vu, Albert Webson, Hyung Won Chung, Yi Tay, Denny Zhou, Quoc V.
 583 Le, Barret Zoph, Jason Wei, and Adam Roberts. The flan collection: Designing data and methods
 584 for effective instruction tuning. *ICML*, 2023.

585

586 Anton Lozhkov, Raymond Li, Loubna Ben Allal, Denis Kocetkov, Chenghao Mou, Christopher Akiki,
 587 Carlos Muñoz Ferrandis, Muennighoff Niklas, Jean Kadour, Yacine Jernite, et al. Starcoder 2 and
 588 the stack v2: The next generation. *arXiv preprint arXiv:2402.19173*, 2024.

589

590 Aman Madaan, Niket Tandon, Prakhar Gupta, Skyler Hallinan, Luyu Gao, Sarah Wiegreffe, Uri Alon,
 591 Nouha Dziri, Shrimai Prabhumoye, Yiming Yang, Sean Welleck, Bodhisattwa Prasad Majumder,
 592 Shashank Gupta, Amir Yazdanbakhsh, and Peter Clark. Self-refine: Iterative refinement with
 593 self-feedback. *arXiv preprint arXiv:2303.17651*, 2023.

594

595 David Mendez, Anna Gaulton, A Patrícia Bento, Jon Chambers, Marleen De Veij, Eloy Félix,
 596 María Paula Magariños, José F Mosquera, Prudence Mutowo, Michał Nowotka, et al. Chembli:
 597 towards direct deposition of bioassay data. *Nucleic Acids Research*, 47(D1):D930–D940, 2019.
 598 doi: 10.1093/nar/gky1075.

594 Remi Munos, Michal Valko, Daniele Calandriello, Mohammad Gheshlaghi Azar, Mark Rowland,
 595 Zhaohan Daniel Guo, Yunhao Tang, Matthieu Geist, Thomas Mesnard, Côme Fiege, Andrea Michi,
 596 Marco Selvi, Sertan Girgin, Nikola Momchev, Olivier Bachem, Daniel J Mankowitz, Doina Precup,
 597 and Bilal Piot. Nash learning from human feedback. In *Proceedings of the 41st International
 598 Conference on Machine Learning*, volume 235 of *Proceedings of Machine Learning Research*, pp.
 599 36743–36768. PMLR, 2024.

600 Arkadi S Nemirovski and David Borisovich Yudin. *Problem Complexity and Method Efficiency in
 601 Optimization*. Wiley-Interscience, New York, 1983.

602

603 Yurii Nesterov and Vladimir Spokoiny. Random gradient-free minimization of convex functions. *Foundations of Computational Mathematics*, 17(2):527–566, 2017. doi: 10.1007/s10208-015-9296-2.

604

605 Allen Nie, Ching-An Cheng, Andrey Kolobov, and Adith Swaminathan. The importance of directional
 606 feedback for ILM-based optimizers. *arXiv preprint arXiv:2405.16434*, 2024.

607

608 Erik Nijkamp, Bo Pang, Hiroaki Hayashi, Lifu Tu, Huan Wang, Yingbo Zhou, Silvio Savarese,
 609 and Caiming Xiong. Codegen: An open large language model for code with multi-turn program
 610 synthesis. *arXiv preprint arXiv:2203.13474*, 2022.

611

612 Marcus Olivecrona, Thomas Blaschke, Ola Engkvist, and Hongming Chen. Molecular de novo
 613 design through deep reinforcement learning. *Journal of Cheminformatics*, 9(1):1–14, 2017. doi:
 10.1186/s13321-017-0235-x.

614

615 OpenAI. Openai o1 system card. Technical report, OpenAI, 2024. URL <https://arxiv.org/abs/2412.16720>.

616

617 Krista Opsahl-Ong, Michael J Ryan, Josh Purtell, David Broman, Christopher Potts, Matei Zaharia,
 618 and Omar Khattab. Optimizing instructions and demonstrations for multi-stage language model
 619 programs. *arXiv preprint arXiv:2406.11695*, 2024.

620

621 Long Ouyang, Jeffrey Wu, Xu Jiang, Diogo Almeida, Carroll Wainwright, Pamela Mishkin, Chong
 622 Zhang, Sandhini Agarwal, Katarina Slama, Alex Ray, John Schulman, Jacob Hilton, Fraser Kelton,
 623 Luke Miller, Maddie Simens, Amanda Askell, Peter Welinder, Paul F Christiano, Jan Leike, and
 624 Ryan Lowe. Training language models to follow instructions with human feedback. *Advances in
 625 Neural Information Processing Systems*, 35:27730–27744, 2022.

626

627 Aaron Parisi, Yao Zhao, and Noah Fiedel. Talm: Tool augmented language models. *arXiv preprint
 628 arXiv:2205.12255*, 2022.

629

630 Reid Pryzant, Dan Iter, Jerry Li, Yin Tat Lee, Chenguang Zhu, and Michael Zeng. Automatic prompt
 631 optimization with “gradient descent” and beam search. *arXiv preprint arXiv:2305.03495*, 2023.

632

633 Valentina Pyatkin, Saumya Malik, Victoria Graf, Hamish Ivison, Shengyi Huang, Pradeep Dasigi,
 634 Nathan Lambert, and Hannaneh Hajishirzi. Generalizing verifiable instruction following. *arXiv
 635 preprint arXiv:2507.02833*, 2025.

636

637 Yujia Qin, Shengding Hu, Yankai Lin, Weize Chen, Ning Ding, Ganqu Cui, Zheni Zeng, Yufei Huang,
 638 Chaojun Xiao, Chi Han, Yi Ren Fung, Yusheng Su, Huadong Wang, Cheng Qian, Runchu Tian,
 639 Kunlun Zhu, Shihao Liang, Xingyu Shen, Bokai Xu, Zhen Zhang, Yining Ye, Bowen Li, Ziwei
 640 Tang, Jing Yi, Yuzhang Zhu, Zhenning Dai, Lan Yan, Xin Cong, Yaxi Lu, Weilin Zhao, Yuxiang
 641 Huang, Junxi Yan, Xu Han, Xian Sun, Dahai Li, Jason Phang, Cheng Yang, Tongshuang Wu,
 642 Heng Ji, Zhiyuan Liu, and Maosong Sun. Tool learning with foundation models. *arXiv preprint
 643 arXiv:2304.08354*, 2023.

644

645 Rafael Rafailov, Archit Sharma, Eric Mitchell, Stefano Ermon, Christopher D Manning, and Chelsea
 646 Finn. Direct preference optimization: Your language model is secretly a reward model. *arXiv
 647 preprint arXiv:2305.18290*, 2023.

648

649 Baptiste Roziere, Jonas Gehring, Fabian Gloeckle, Sten Sootla, Itai Gat, Xiaoqing Ellen Tan, Yossi
 650 Adi, Jingyu Liu, Tal Remez, Jérémie Rapin, Artyom Kozhevnikov, Ivan Evtimov, Joanna Bitton,
 651 Manish Bhatt, Cristian Canton Ferrer, Aaron Grattafiori, Wenhan Xiong, Alexandre Défossez, Jade
 652 Copet, Faisal Azhar, Hugo Touvron, Louis Martin, Nicolas Usunier, Thomas Scialom, and Gabriel
 653 Synnaeve. Code llama: Open foundation models for code. *arXiv preprint arXiv:2308.12950*, 2023.

648 William Saunders, Catherine Yeh, Jeff Wu, Steven Bills, Long Ouyang, Jonathan Ward, and Jan
 649 Leike. Self-critiquing models for assisting human evaluators. *arXiv preprint arXiv:2206.05802*,
 650 2022.

651 Jérémie Scheurer, Jon Ander Campos, Jun Shern Chan, Angelica Chen, Kyunghyun Cho, and Ethan
 652 Perez. Training language models with language feedback at scale. *arXiv preprint arXiv:2303.16755*,
 653 2023.

654 Timo Schick, Jane Dwivedi-Yu, Roberto Dessì, Roberta Raileanu, Maria Lomeli, Luke Zettlemoyer,
 655 Nicola Cancedda, and Thomas Scialom. Peer: A collaborative language model. *arXiv preprint*
 656 *arXiv:2208.11663*, 2022.

657 Timo Schick, Jane Dwivedi-Yu, Roberto Dessì, Roberta Raileanu, Maria Lomeli, Luke Zettlemoyer,
 658 Nicola Cancedda, and Thomas Scialom. Toolformer: Language models can teach themselves to
 659 use tools. *NeurIPS*, 2023.

660 Zhihong Shao, Peiyi Wang, Qihao Zhu, Runxin Xu, Junxiao Song, Xiao Bi, Haowei Zhang,
 661 Mingchuan Zhang, YK Li, Yang Wu, et al. Deepseekmath: Pushing the limits of mathematical
 662 reasoning in open language models. *arXiv preprint arXiv:2402.03300*, 2024.

663 David Silver and Richard S. Sutton. Welcome to the era of experience. In *Designing an Intelligence*.
 664 MIT Press, 2025. Preprint.

665 Charlie Snell, Jaehoon Lee, Kelvin Xu, and Aviral Kumar. Scaling llm test-time compute optimally
 666 can be more effective than scaling model parameters. *arXiv preprint arXiv:2408.03314*, 2024.

667 Tianxiang Sun, Zhengfu Chen, Xipeng Qiu, and Xuanjing Huang. Bbtv2: Towards a gradient-free
 668 future with large language models. *arXiv preprint arXiv:2205.11200*, 2022.

669 The UniProt Consortium. Uniprot: the universal protein knowledgebase in 2023. *Nucleic Acids
 670 Research*, 51(D1):D523–D531, 2023. doi: 10.1093/nar/gkac1052.

671 Austin Tripp, Gregor N. C. Simm, and José Miguel Hernández-Lobato. A fresh look at de novo
 672 molecular design benchmarks. In *NeurIPS 2021 AI for Science Workshop*, 2021. URL https://openreview.net/forum?id=gS3XMun4cl_.

673 Jiayi Wang, Yuxuan Sun, Wenjia Zhang, et al. Adaptive preference scaling for reinforcement learning
 674 with human feedback. *arXiv preprint arXiv:2406.02764*, 2024.

675 Lei Wang, Chen Ma, Xueyang Feng, Zeyu Zhang, Hao Yang, Jingsen Zhang, Zhiyuan Chen, Jiakai
 676 Tang, Xu Chen, Yankai Lin, et al. A survey on large language model based autonomous agents.
 677 *arXiv preprint arXiv:2308.11432*, 2023a.

678 Yue Wang, Hung Le, Akhilesh Deepak Gotmare, Nghi D.Q. Bui, Junnan Li, and Steven C.H. Hoi.
 679 Codet5+: Open code large language models for code understanding and generation. *Proceedings
 680 of EMNLP*, 2023b.

681 Jason Wei, Maarten Bosma, Vincent Y. Zhao, Kelvin Guu, Adams Wei Yu, Brian Lester, Nan Du,
 682 Andrew M. Dai, and Quoc V. Le. Finetuned language models are zero-shot learners. *ICLR*, 2022a.

683 Jason Wei, Xuezhi Wang, Dale Schuurmans, Maarten Bosma, Brian Ichter, Fei Xia, Ed H. Chi,
 684 Quoc V. Le, and Denny Zhou. Chain-of-thought prompting elicits reasoning in large language
 685 models. In *NeurIPS*, 2022b.

686 David Weininger. Smiles, a chemical language and information system. 1. introduction to methodol-
 687 ogy and encoding rules. *Journal of Chemical Information and Computer Sciences*, 28(1):31–36,
 688 1988. doi: 10.1021/ci00057a005.

689 Sean Welleck, Ximing Lu, Peter West, Faiz Karim, Liwei Jiang, Khyathi Chandu, Nouha Dziri,
 690 Ronan Le Bras, Lianhui Qin, Yu Gu, Rachel Rudinger, and Yejin Choi. Generating sequences by
 691 learning to self-correct. *ICLR*, 2023.

692 Christian Wirth, Riad Akour, Gerhard Neumann, and Johannes Fürnkranz. A survey of preference-
 693 based reinforcement learning methods. *Journal of Machine Learning Research*, 18(136):1–46,
 694 2017.

702 Wei Xiong, Hanze Dong, Chenlu Ye, Han Zhong, Nan Jiang, and Tong Zhang. Iterative preference
703 learning from human feedback: Bridging theory and practice for rlhf under kl-constraint. *arXiv*
704 *preprint arXiv:2312.11456*, 2023.

705 Chengrun Yang, Xuezhi Wang, Yifeng Lu, Hanxiao Liu, Quoc V. Le, Denny Zhou, and Xinyun Chen.
706 Large language models as optimizers. *arXiv preprint arXiv:2309.03409*, 2023.

708 Shunyu Yao, Dian Yu, Jeffrey Zhao, Izhak Shafran, Thomas L. Griffiths, Yuan Cao, and Karthik
709 Narasimhan. Tree of Thoughts: Deliberate problem solving with large language models. 2023a.

710 Shunyu Yao, Jeffrey Zhao, Dian Yu, Nan Du, Izhak Shafran, Karthik Narasimhan, and Yuan Cao.
711 React: Synergizing reasoning and acting in language models. *ICLR*, 2023b.

713 Mert Yuksekgonul, Federico Bianchi, Joseph Boen, Sheng Liu, Pan Lu, Zhi Huang, Carlos Guestrin,
714 and James Zou. Textgrad: Automatic "differentiation" via text. *arXiv preprint arXiv:2406.07496*,
715 2024.

716 Eric Zelikman, Yuhuai Wu, Jesse Mu, and Noah D. Goodman. Star: Bootstrapping reasoning with
717 reasoning. *arXiv preprint arXiv:2203.14465*, 2022.

719 Shengyu Zhang, Linfeng Dong, Xiaoya Li, Sen Zhang, Xiaofei Sun, Shuhe Wang, Jiwei Li, Runyi
720 Hu, Tianwei Zhang, Fei Wu, et al. Instruction tuning for large language models: A survey. *arXiv*
721 *preprint arXiv:2308.10792*, 2024.

722 Xiang Zhou, Yuxuan Liu, Zhiyuan Chen, et al. Towards thinking-optimal scaling of test-time compute
723 for llm reasoning. *arXiv preprint arXiv:2502.18080*, 2025.

725 Yongchao Zhou, Andrei Ioan Muresanu, Ziwen Han, Keiran Paster, Silviu Pitis, Harris Chan,
726 and Jimmy Ba. Large language models are human-level prompt engineers. *arXiv preprint*
727 *arXiv:2211.01910*, 2022.

728 Qihao Zhu, Daya Guo, Zhihong Shao, Dejian Yang, Peiyi Wang, Runxin Xu, Y Wu, Yukun Li,
729 Huazuo Gao, Shirong Ma, et al. Deepseek-coder-v2: Breaking the barrier of closed-source models
730 in code intelligence. *arXiv preprint arXiv:2406.11931*, 2024.

731

732

733

734

735

736

737

738

739

740

741

742

743

744

745

746

747

748

749

750

751

752

753

754

755

756 A FORMAL STATEMENTS AND PROOFS
757758 **Proposition 1** (Linear convergence under PL with rationale-guided directions). *Let $r : Z \rightarrow \mathbb{R}$ be
759 L -smooth and satisfy the μ -PL condition (for maximization)*

760
$$\frac{1}{2} \|\nabla r(z)\|_2^2 \geq \mu(r(z^*) - r(z)) \quad \forall z \in Z.$$

761
762

763 At iteration t , suppose a direction v_t satisfies

764
$$\mathbb{E}[v_t | z_t] = \alpha \nabla r(z_t), \quad \mathbb{E}[\|v_t - \mathbb{E}[v_t | z_t]\|_2^2 | z_t] \leq \sigma^2 \|\nabla r(z_t)\|_2^2,$$

765

766 with constants $\alpha > 0$ and $\sigma \geq 0$, and define $\kappa_1 \triangleq \alpha^2 + \sigma^2$. Consider the update $z_{t+1} = z_t + \eta v_t$.
767 If a constraint set Z is present, assume $z_t + \eta v_t \in Z$ (i.e., the projection is inactive). With stepsize
768 $\eta = \alpha/(L\kappa_1)$,

769
$$\mathbb{E}[r(z^*) - r(z_{t+1}) | z_t] \leq \left(1 - \frac{\mu\alpha^2}{L\kappa_1}\right) [r(z^*) - r(z_t)].$$

770

771 Unrolling yields

772
$$\mathbb{E}[r(z^*) - r(z_T)] \leq \left(1 - \frac{\mu\alpha^2}{L\kappa_1}\right)^T [r(z^*) - r(z_0)],$$

773

774 so ϵ -accuracy is achieved in

775
$$T = O\left(\frac{L(\alpha^2 + \sigma^2)}{\mu\alpha^2} \log \frac{1}{\epsilon}\right)$$

776

777 iterations.

779 *Proof.* L -smoothness gives the two-sided bound
780

781
$$r(z_t + \eta v_t) \geq r(z_t) + \eta \langle \nabla r(z_t), v_t \rangle - \frac{L}{2} \eta^2 \|v_t\|_2^2.$$

782 Taking conditional expectation and using $\mathbb{E}[v_t | z_t] = \alpha \nabla r(z_t)$ and $\mathbb{E}[\|v_t\|_2^2 | z_t] \leq (\alpha^2 +$
783 $\sigma^2) \|\nabla r(z_t)\|_2^2 = \kappa_1 \|\nabla r(z_t)\|_2^2$,

784
$$\mathbb{E}[r(z_{t+1}) | z_t] \geq r(z_t) + \left(\eta\alpha - \frac{L}{2}\eta^2\kappa_1\right) \|\nabla r(z_t)\|_2^2.$$

785

787 By the PL inequality, $\|\nabla r(z_t)\|_2^2 \geq 2\mu[r(z^*) - r(z_t)]$, so
788

789
$$\mathbb{E}[r(z^*) - r(z_{t+1}) | z_t] \leq \left(1 - 2\mu\eta\alpha + \mu L\eta^2\kappa_1\right) [r(z^*) - r(z_t)].$$

790

791 Choosing $\eta = \alpha/(L\kappa_1)$ makes the bracket equal to $1 - \mu\alpha^2/(L\kappa_1)$, yielding the claim. \square
792

793 A.1 QUERY COMPLEXITY AND DIMENSION DEPENDENCE

794 **Dimension-Free Case.** When rationales provide full gradient information ($v_t \in \mathbb{R}^d$) at unit cost, the
795 query complexity equals T and is dimension-independent:

796
$$\text{Queries} = O\left(\frac{L(\alpha^2 + \sigma^2)}{\alpha^2\mu} \log \frac{1}{\epsilon}\right) \quad (3)$$

797
798

800 **Coordinate-Sparse Case.** Suppose each query reveals one coordinate of $\nabla r(z_t)$ chosen uniformly
801 at random. Using the unbiased estimator $v_t = d(\partial_i r(z_t)) e_i$ with $i \sim \text{Unif}([d])$ gives $\alpha = 1$,
802 $\sigma^2 = d - 1$, and hence $\kappa_1 = d$ and stepsize $\eta = 1/(Ld)$. We have

803
$$T = O\left(\frac{Ld}{\mu} \log \frac{1}{\epsilon}\right), \quad \text{Queries} = O\left(\frac{Ld}{\mu} \log \frac{1}{\epsilon}\right).$$

804
805

806 Equivalently, averaging m independent coordinate queries per iteration yields $\sigma^2 = (d - 1)/m$;
807 taking $m = d$ recovers $T = O((L/\mu) \log(1/\epsilon))$ with d queries per iteration, so total queries remain
808 $\Theta\left(\frac{Ld}{\mu} \log \frac{1}{\epsilon}\right)$.
809

810 This clarifies when and why dimension appears in the complexity.

810 B LOWER BOUNDS FOR EXHAUSTIVE/RANDOM ZEROTH-ORDER SEARCH
811812 We formalize the intrinsic slowness of exhaustive (grid) search and best-of- N random sampling when
813 only function values (or preferences) are used without directional information. The hard instance is
814 the strongly concave quadratic

815
$$r(z) = r(z^*) - \frac{\mu}{2} \|z - z^*\|_2^2, \quad z \in B_R(z^*) \subset \mathbb{R}^d,$$

816

817 whose ϵ -optimal set is the ball $B_{\rho_\epsilon}(z^*)$ with radius $\rho_\epsilon = \sqrt{2\epsilon/\mu}$.818 **Proposition 2** (Grid-search lower bound). *Let $B_R(z^*) \subset \mathbb{R}^d$ and a hypercubic grid of spacing h . Its
819 covering radius is $\rho = \frac{\sqrt{d}h}{2}$. To guarantee that for all placements of z^* there exists a grid point in the
820 ϵ -optimal ball $B_{\rho_\epsilon}(z^*)$ with $\rho_\epsilon = \sqrt{2\epsilon/\mu}$, it suffices that $\rho \leq \rho_\epsilon$ (i.e., $h \leq 2\rho_\epsilon/\sqrt{d}$). Furthermore,
821 any such grid restricted to $B_R(z^*)$ must contain at least*

822
$$N \geq \left(\frac{R}{\rho}\right)^d = \left(\frac{R\sqrt{d}}{2\rho_\epsilon}\right)^d = \left(\frac{\mu R^2 d}{8\epsilon}\right)^{d/2}$$

823

824 points. Hence exhaustive grid search is exponential in d and polynomial in $1/\epsilon$ with exponent $d/2$ on
825 this family.826 *Proof.* Coverage of $B_R(z^*)$ by N balls of radius ρ centered at grid points implies $NV_d\rho^d \geq V_dR^d$,
827 hence $N \geq (R/\rho)^d$. With $\rho = \sqrt{d}h/2$ and $h \leq 2\rho_\epsilon/\sqrt{d}$, we obtain $N \geq (R\sqrt{d}/(2\rho_\epsilon))^d$. Substitute
828 $\rho_\epsilon = \sqrt{2\epsilon/\mu}$ to conclude. \square 829 **Proposition 3** (Best-of- N random sampling lower bound). *Draw $X_1, \dots, X_N \stackrel{i.i.d.}{\sim} \text{Unif}(B_R(z^*))$ and let $\hat{z} = \arg \max_i r(X_i)$ for $r(z) = r(z^*) - \frac{\mu}{2}\|z - z^*\|_2^2$. Then with $a \triangleq 2/d$,*

830
$$\mathbb{E}[r(z^*) - r(\hat{z})] = \frac{\mu R^2}{2} N \text{B}(1+a, N) = \frac{\mu R^2}{2} \Gamma(1+a) \frac{\Gamma(N+1)}{\Gamma(N+1+a)}.$$

831

832 Moreover, for all $d \geq 1$ (so $a \in (0, 2]$),

833
$$\frac{\Gamma(N+1)}{\Gamma(N+1+a)} \geq (N+2)^{-a},$$

834

835 and thus

836
$$\mathbb{E}[r(z^*) - r(\hat{z})] \geq \frac{\mu R^2}{2} \Gamma\left(1 + \frac{2}{d}\right) (N+2)^{-\frac{2}{d}} = \Omega(N^{-\frac{2}{d}}).$$

837

838 *Proof.* Let $R_i = \|X_i - z^*\|_2$ and $R_{\min} = \min_i R_i$. The CDF of R_{\min} is $F(r) = 1 - (1 - (r/R)^d)^N$
839 for $r \in [0, R]$. Differentiating, $f(r) = Ndr^{d-1}R^{-d}(1 - (r/R)^d)^{N-1}$. Then

840
$$\mathbb{E}[R_{\min}^2] = \int_0^R r^2 f(r) dr = NR^2 \int_0^1 t^{\frac{2}{d}} (1-t)^{N-1} dt = NR^2 \text{B}\left(1 + \frac{2}{d}, N\right),$$

841

842 where $t = (r/R)^d$ and B is the Beta function. Using $\text{B}(a, b) = \frac{\Gamma(a)\Gamma(b)}{\Gamma(a+b)}$ gives the exact expression.
843 For the bound, we use the inequality $\Gamma(N+1)/\Gamma(N+1+a) \geq (N+2)^{-a}$ which holds for all
844 $a \in (0, 2]$ and $N \geq 1$. \square 845 C EXTENDED EXPERIMENT SECTION
846

847 C.1 IMPLEMENTATION DETAILS

848 **SVG Code Optimization.** We employ a tournament-style approach where `gpt-5-mini` generates
849 SVG/TikZ code that gets rendered to PNG images for pairwise aesthetic comparisons by a separate
850 instance of the same model acting as judge. The system maintains a “champion” design that only
851 updates when both A-vs-B and B-vs-A orderings consistently agree on a winner, accumulating
852 winning rationales into the generation prompt to guide aesthetic improvements across iterations. The
853 judge provides natural language rationales explaining aesthetic preferences that inform subsequent
854 generations.

	Method	ADRB1	PGR	PPARA	PPARG	CDK2	F2
864 DOCKSTRING (N=260155)	Top 50%	5.305	3.478	4.549	4.210	4.385	4.168
	Top 90%	8.785	7.878	7.987	7.658	7.733	7.477
	Top 99%	9.620	8.703	8.718	8.449	8.453	8.139
	Top 99.9%	10.209	9.260	9.230	9.012	8.979	8.722
	Top 99.99%	<u>10.742</u>	<u>9.723</u>	9.821	9.518	9.509	9.252
	Best Molecule	<u>11.330</u>	<u>9.742</u>	9.907	9.529	9.534	9.311
	GP-BO [†]	10.552 ± 0.140	9.307 ± 0.177	9.680 ± 0.337	9.485 ± 0.279	9.067 ± 0.289	8.686 ± 0.068
865	Graph MCTS [†]	8.883 ± 0.826	7.819 ± 0.319	7.363 ± 0.935	7.134 ± 0.855	7.777 ± 0.723	6.310 ± 0.704
866	Graph GA [†]	10.249 ± 1.002	8.793 ± 0.497	9.211 ± 0.343	8.769 ± 0.432	8.652 ± 0.449	8.900 ± 0.817
867	SMILES GA	9.334 ± 0.237	8.335 ± 0.276	9.052 ± 0.484	8.560 ± 0.346	8.268 ± 0.170	7.984 ± 0.554
868	REINVENT	9.867 ± 0.522	8.604 ± 0.483	8.735 ± 0.120	9.054 ± 0.153	8.695 ± 0.370	8.441 ± 0.535
869	No Feedback (Best-of-N)	6.190 ± 0.821	8.619 ± 0.562	8.230 ± 0.628	8.633 ± 0.549	8.300 ± 0.620	8.793 ± 0.921
870	Random Feedback	6.604 ± 0.577	8.385 ± 0.258	8.276 ± 0.628	6.780 ± 0.523	8.793 ± 0.921	7.993 ± 0.663
871	Minimal Feedback	5.863 ± 0.428	8.779 ± 0.633	8.507 ± 0.428	7.998 ± 0.571	9.439 ± 0.922	8.420 ± 0.315
872	TextGrad	8.531 ± 0.278	8.057 ± 0.383	7.953 ± 0.160	7.256 ± 0.886	8.174 ± 0.395	7.357 ± 0.821
873	Feedback Descent	10.623 ± 0.112	9.615 ± 0.158	9.919 ± 0.305	10.187 ± 0.253	9.803 ± 0.267	9.300 ± 0.062
874							

Table 4: Full results for molecule optimization on six protein targets. For each target, the top generative result is in **bold**, and any population in the DOCKSTRING database that exceeds the best generative result is underlined. **Feedback Descent** rivals or surpasses specialized molecular optimizers across all six targets.

IFBench Prompt Optimization. We closely follow the setting of [Agrawal et al. \(2025\)](#) for this experiment. We use their two-stage DSPy program with the `gpt-4.1-mini` model and temperature 1.0 for the solver and 0.0 for proposer/tagger to balance exploration and precision. To compare two prompts, we go through the training set to identify examples where program A succeeds and B fails, A fails and B succeeds, both fail, or both succeed, creating four explicit quadrants for analysis. We compute lift and precision/recall metrics on hypothesis tags, where lift measures the base rate of each event and the rate at which it occurs under a subset.

Molecule Optimization. We implement molecular optimization using the DOCKSTRING package ([García-Ortegón et al., 2022](#)) for protein-ligand docking simulations across six therapeutic targets. The system begins with three simple seed molecules (acetamide, pentane, benzene) and progressively evolves SMILES strings through iterative feedback loops that incorporate RDKit molecular properties, protein binding site information, and similarity comparisons to approved drugs as metadata. We use the combined score function suggested by DOCKSTRING:

$$s_{\text{overall}}(\text{molecule, protein}) = -\text{Vina}(\text{molecule, protein}) - 10 * (1 - \text{QED}(\text{molecule})), \quad (4)$$

where `Vina` provides the binding affinity prediction (kcal/mol, more negative is better) and the QED penalty term penalizes molecules with poor drug-likeness, with lower overall scores indicating better molecules that balance binding strength and drug-like properties. Note that QED scores range from 0 to 1 while `Vina` scores typically range from -3.0 to -12.0 kcal/mol. For Feedback Descent, we use a batch size of 8 and top-k selection of 10 examples.

C.2 ADDITIONAL RESULTS

[Fig. 6](#) shows that across all protein targets, the discovered molecules extend beyond the DOCKSTRING baseline along both axes. The resulting Pareto frontiers illustrate consistent improvements in the joint trade-off between docking affinity and drug-likeness, highlighting that feedback-guided search yields coordinated gains rather than isolated outliers.

[Fig. 7](#) shows optimization trajectories across all six protein targets. In each case, Feedback Descent reaches strong binding scores within the first few hundred oracle calls, while the competing specialized methods often plateau early (e.g., GRAPH-MCTS) or require substantially more evaluations to approach similar performance (e.g., SMILES-GA, GP-BO). Overall, the method is competitive with these baselines and in several cases outperforms them, suggesting that textual feedback provides a broadly effective and robust optimization signal across diverse binding targets.

C.3 PROMPT TEMPLATES

We use the following prompt for the judge for the Anatomy SVG task. The rubrics for the other tasks are written in a similar style, translating a particular aesthetic into operational rules that minimize ambiguity.

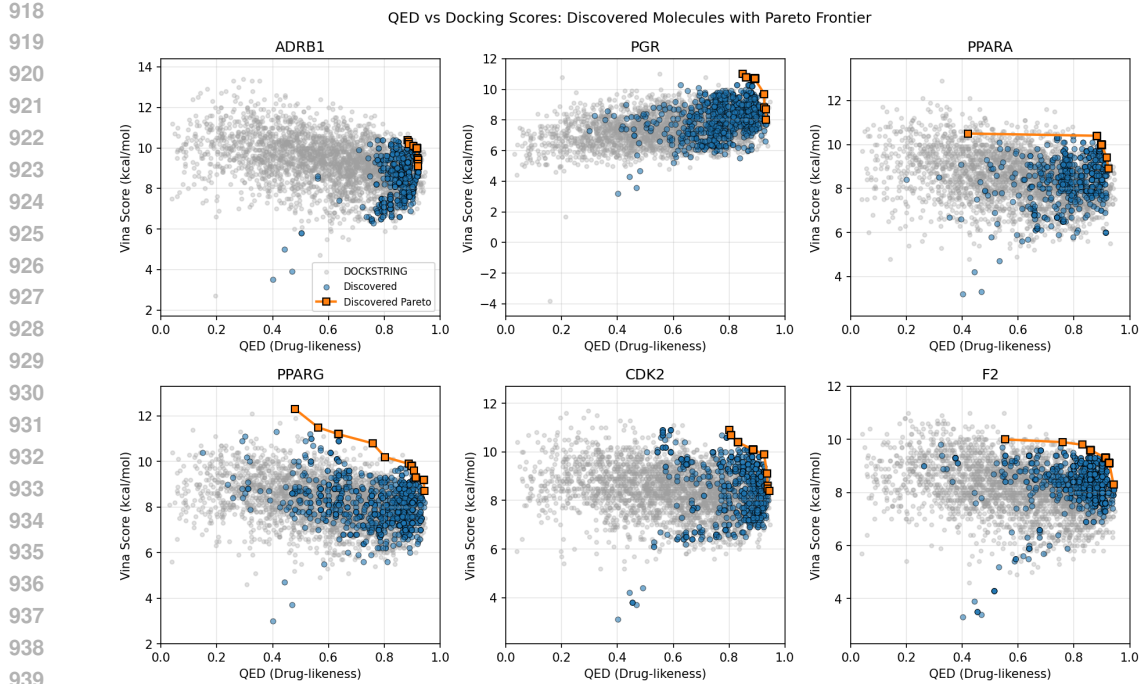


Figure 6: Pareto frontiers of discovered molecules (blue) compared against molecules in the DOCKSTRING dataset (gray) across six protein targets. The highlighted orange markers indicate molecules on the discovered Pareto frontier, achieving joint improvements in docking affinity (Vina score) and drug-likeness (QED).

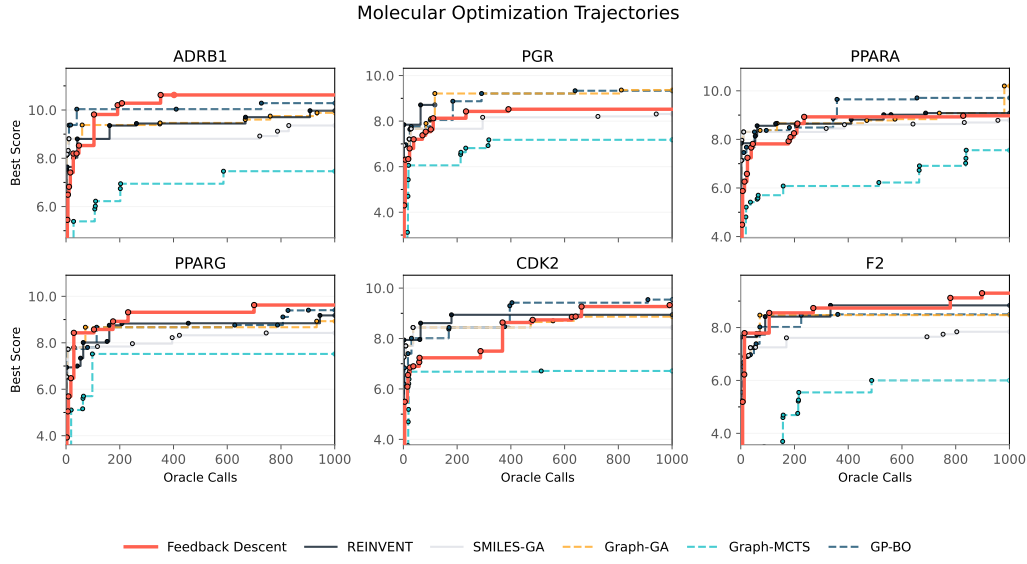


Figure 7: **Optimization trajectories across six protein targets.** Feedback Descent consistently attains higher docking scores with fewer oracle calls compared to standard molecular optimization baselines (REINVENT, SMILES-GA, GRAPH-GA, GRAPH-MCTS, GP-BO).

Anatomy Judge Rubric

RUBRIC NAME: Anatomical Realism

```

972
973 INTENT: Believable equine anatomy with a plausible horn; form,
974 proportion, and structure matter most.
975
976 NON-NEGOTIABLES:
977 - Recognizable equine proportions; head, neck, torso, four legs, mane
978 , tail, horn present.
979 - Limbs connect anatomically; joints and hooves indicated.
980
981 CRITICAL BENCHMARKS (must evaluate these first):
982 1. Head-Neck Proportion: Neck length should be ~1.5x head length;
983 head meets neck high on shoulders
984 2. Body Square: Body length (shoulder to buttock) ~ height at withers
985 ; chest depth ~ elbow height
986 3. Leg Structure: Proper joint articulation with elbow under withers;
987 fetlock/pastern angles 45-55 deg when standing; all four limbs
988 distinct and correctly connected
989
990 WHAT TO REWARD:
991 - Correct limb count and articulation; mass distribution that could
992 stand or move.
993 - Horn integrates naturally with the skull (frontal bone center, 2-3"
994 above eye line).
995 - Subtle shading or line variation conveying volume.
996 - Ground contact or cast shadow for grounding.
997 - Visible muscle definition suggesting tension/relaxation appropriate
998 to pose.
999 - Differentiated hair textures: short coat vs coarse mane/tail
1000 strands.
1001 - Anatomical landmarks: withers prominence, gaskin curve.
1002
1003 WHAT TO PENALIZE:
1004 - Missing or fused legs; impossible joints; balloon torsos.
1005 - Flat cardboard profiles with no sense of volume.
1006 - Decorative effects that obscure structure.
1007 - Disney-fied proportions (oversized eyes, baby-like features).
1008 - Horn placement anywhere except frontal bone center (2-3" above eye
1009 line).
1010
1011 TIEBREAKERS:
1012 - Prefer the image with more accurate limb/neck/head proportions.
1013 - If both are plausible, choose the one with better weight and
1014 grounding.
1015
1016
1017
1018
1019
1020
1021
1022
1023
1024
1025

```

1009
1010 We use the following prompt templates for candidate generation and rationale generation for prompt
1011 optimization.

1012 Prompt Template IFBench Candidate Generation

```

1013
1014 You are tasked with improving an assistant's prompt based on task
1015 data, examples, and feedback.
1016
1017 ## Current Prompts
1018 **Approach A (Baseline):**
1019 ````python
1020 {prompt_a_dict}
1021 ````

1022 **Approach B (Challenger):**
1023 ````python
1024 {prompt_b_dict}
1025 ````
```

```

1026
1027
1028     ## Training Signals
1029     {comparison}
1030
1031     ## Step 1: Task Inference
1032     - Read the examples and feedback carefully.
1033     - Infer the underlying task structure, required input/output forms,
1034     and success criteria.
1035     - Identify implicit constraints not explicitly stated in the original
1036     prompts.
1037
1038     ## Step 2: Knowledge Preservation
1039     - Extract and encode domain-specific facts, constraints, and
1040     conventions discovered in the examples.
1041     - Include niche technical details that may not be obvious to a model
1042     without this context.
1043     - Distill general strategies the assistant used successfully.
1044
1045     ## Step 3: Failure Analysis
1046     - Identify recurring mistakes and failure modes.
1047     - Devise principle-based instructions to avoid them.
1048     - When both approaches fail on a pattern, invent a new, generalizable
1049     strategy.
1050
1051     ## Step 4: Prompt Synthesis
1052     Write a new instruction prompt that:
1053     1. Captures the task understanding (Step 1).
1054     2. Preserves domain-specific facts (Step 2).
1055     3. Embeds strategies that worked and guards against failures (Step 3)
1056     .
1057     4. Remains SHORT, PRINCIPLE-BASED, and free of training-set
1058     overfitting.
1059     5. Works robustly on UNSEEN TEST DATA.
1060
1061     The prompt must be a Python dictionary with the following keys:
1062     {module_keys_description}
1063
1064     Output EXACTLY in this format:
1065
1066     ````python
1067     {prompt_template}
1068     ```````
1069
1070     You are improving {artifact_type}. Here is the previous feedback:
1071
1072     Iteration 1: {rationale_1}
1073     Iteration 2: {rationale_2}
1074     ...
1075     Iteration {n}: {rationale_n}
1076
1077     Current best version:
1078     {current_best}
1079
1080     Generate an improved version that addresses the feedback while
1081     preserving existing strengths. Focus on the most actionable
1082     suggestions from the rationales above.

```

Prompt Template for Molecule Optimization

1076

1077 You are a helpful assistant that proposes a single SMILES string
1078 corresponding to a small molecule, based on the task explanation and
1079 information about previous molecules that have been proposed. Your

```

1080
1081 proposed molecule should score highly on the {benchmark_name}
1082 benchmark.
1083 Task explanation: Maximize -{benchmark_name} - 10 * (1 - QED): larger
1084 values mean stronger {benchmark_name} binding and high drug-likeness
1085 .
1086 {protein_info_xml}
1087 Your output format should be EXACTLY as follows:
1088
1089 <reasoning>[Chemical hypothesis linking structural changes to
1090 expected binding/QED improvements]</reasoning>
1091 <smiles>[Single SMILES string]</smiles>
1092
1093 Generate a small molecule based on these previous examples (sorted in
1094 descending order of score):
1095
1096 {examples_text}
1097

```

Example of Protein Metadata (ADRB1)

```

1100 { 'target': 'ADRB1', 'accession': 'P08588', 'regions': {
1101   'transmembrane': [[56, 84], [94, 120], [133, 154], [173, 196], [223,
1102   248], [320, 349], [355, 377]], 'extracellular': [[1, 55], [121, 132],
1103   [197, 222], [350, 354]], 'cytoplasmic': [[85, 93], [155, 172], [249,
1104   319], [378, 477]], 'disordered': [[269, 307], [403, 477]]}, 'critical_residues': {'mutagenesis': [{'position': [474, 474], 'description': 'Loss of interaction with GOPC.'}, {'position': [474, 474], 'description': 'Loss of interaction with GOPC; when associated with A-477.'}, {'position': [475, 475], 'description': 'Loss of interaction with GOPC. Loss of interaction with RAPGEF2. Abolishes agonist-induced Ras activation.'}, {'position': [475, 475], 'description': 'Loss of interaction with RAPGEF2.'}, {'position': [475, 475], 'description': 'Partial loss of interaction with GOPC.'}, {'position': [476, 476], 'description': 'Partial loss of interaction with GOPC.'}, {'position': [477, 477], 'description': 'Loss of interaction with GOPC.'}, {'position': [477, 477], 'description': 'Loss of interaction with RAPGEF2. Abolishes agonist-induced Ras activation.'}], 'natural_variants': [{'position': [26, 26], 'description': 'in dbSNP:rs34844626'}, {'position': [29, 29], 'description': 'in dbSNP:rs35720093'}, {'position': [31, 31], 'description': 'in dbSNP:rs35230616'}, {'position': [49, 49], 'description': 'correlated with low mean resting heart rate and decreased mortality risk in patients with congestive heart failure; dbSNP:rs1801252'}, {'position': [187, 187], 'description': 'found in individuals with short sleep; results in decreased adenylyl cyclase-activating adrenergic receptor signaling; decreased protein stability; dbSNP:rs776439595'}, {'position': [389, 389], 'description': 'increased betal-adrenergic receptor activity; increased basal activity and increased coupling to heterotrimeric G protein Gs that stimulates the adenylyl cyclase; dbSNP:rs1801253'}, {'position': [399, 399], 'description': 'in dbSNP:rs36052953'}, {'position': [405, 405], 'description': 'in dbSNP:rs35705839'}]}}
1127
1128

```

Example of Molecule Metadata (CCCCC)

```

1130 valid: 'True'
1131 score: '-1.9121449019886678'
1132 metadata:
1133

```

```

1134 CanonicalSMILES: CCCCC
1135 InChIKey: OFBQJSOFQDEBGM-UHFFFAOYSA-N
1136 MolecularFormula: C5H12
1137 ExactMass: '72.093900384'
1138 FormalCharge: '0'
1139 AtomCount: '5'
1140 HeavyAtomCount: '5'
1141 HeteroAtomCount: '0'
1142 BondCount: '4'
1143 Sp3CarbonFraction: '1.0'
1144 RingCount: '0'
1145 AromaticRingCount: '0'
1146 AliphaticRingCount: '0'
1147 RotatableBondCount: '2'
1148 StereoCenterCount: '0'
1149 MurckoScaffold: ''
1150 LogP: '2.1965000000000003'
1151 TopologicalPolarSurfaceArea: '0.0'
1152 MolarRefractivity: '25.19899999999999'
1153 HBondDonorCount: '0'
1154 HBondAcceptorCount: '0'
1155 BertzComplexityIndex: '7.5097750043269365'
1156 BalabanJIndex: 2.19060968716425
1157 HallKierAlpha: '0.0'
1158 Kappa1: '5.0'
1159 Chi0v: '4.121320343559642'
1160 TotalEState: 8.5
1161 MinEState: 1.34375
1162 MaxEState: 2.2118055555555554
1163 PEOE_VSA6: '33.10993926815928'
1164 SlogP_VSA5: '33.10993926815928'
1165 BCUTp_1h: '13.744962415414642'
1166 AccessibleSurfaceArea: '34.19901948541599'
1167 FunctionalGroups: []
1168 StructuralAlerts: []
1169 QuantitativeDrugLikeness: '0.4687855098011332'
1170 SyntheticAccessibility: '1.699621281696647'
1171 NaturalProductLikeness: '0.09749981667944'
1172
1173
1174
1175
1176
1177
1178
1179
1180
1181
1182
1183
1184
1185
1186
1187
1188
1189
1190
1191
1192
1193
1194
1195
1196
1197
1198
1199
1200
1201
1202
1203
1204
1205
1206
1207
1208
1209
1210
1211
1212
1213
1214
1215
1216
1217
1218
1219
1220
1221
1222
1223
1224
1225
1226
1227
1228
1229
1230
1231
1232
1233
1234
1235
1236
1237
1238
1239
1240
1241
1242
1243
1244
1245
1246
1247
1248
1249
1250
1251
1252
1253
1254
1255
1256
1257
1258
1259
1260
1261
1262
1263
1264
1265
1266
1267
1268
1269
1270
1271
1272
1273
1274
1275
1276
1277
1278
1279
1280
1281
1282
1283
1284
1285
1286
1287
1288
1289
1290
1291
1292
1293
1294
1295
1296
1297
1298
1299
1300
1301
1302
1303
1304
1305
1306
1307
1308
1309
1310
1311
1312
1313
1314
1315
1316
1317
1318
1319
1320
1321
1322
1323
1324
1325
1326
1327
1328
1329
1330
1331
1332
1333
1334
1335
1336
1337
1338
1339
1340
1341
1342
1343
1344
1345
1346
1347
1348
1349
1350
1351
1352
1353
1354
1355
1356
1357
1358
1359
1360
1361
1362
1363
1364
1365
1366
1367
1368
1369
1370
1371
1372
1373
1374
1375
1376
1377
1378
1379
1380
1381
1382
1383
1384
1385
1386
1387
1388
1389
1390
1391
1392
1393
1394
1395
1396
1397
1398
1399
1400
1401
1402
1403
1404
1405
1406
1407
1408
1409
1410
1411
1412
1413
1414
1415
1416
1417
1418
1419
1420
1421
1422
1423
1424
1425
1426
1427
1428
1429
1430
1431
1432
1433
1434
1435
1436
1437
1438
1439
1440
1441
1442
1443
1444
1445
1446
1447
1448
1449
1450
1451
1452
1453
1454
1455
1456
1457
1458
1459
1460
1461
1462
1463
1464
1465
1466
1467
1468
1469
1470
1471
1472
1473
1474
1475
1476
1477
1478
1479
1480
1481
1482
1483
1484
1485
1486
1487
1488
1489
1490
1491
1492
1493
1494
1495
1496
1497
1498
1499
1500
1501
1502
1503
1504
1505
1506
1507
1508
1509
1510
1511
1512
1513
1514
1515
1516
1517
1518
1519
1520
1521
1522
1523
1524
1525
1526
1527
1528
1529
1530
1531
1532
1533
1534
1535
1536
1537
1538
1539
1540
1541
1542
1543
1544
1545
1546
1547
1548
1549
1550
1551
1552
1553
1554
1555
1556
1557
1558
1559
1560
1561
1562
1563
1564
1565
1566
1567
1568
1569
1570
1571
1572
1573
1574
1575
1576
1577
1578
1579
1580
1581
1582
1583
1584
1585
1586
1587
1588
1589
1590
1591
1592
1593
1594
1595
1596
1597
1598
1599
1599
1600
1601
1602
1603
1604
1605
1606
1607
1608
1609
1610
1611
1612
1613
1614
1615
1616
1617
1618
1619
1620
1621
1622
1623
1624
1625
1626
1627
1628
1629
1630
1631
1632
1633
1634
1635
1636
1637
1638
1639
1640
1641
1642
1643
1644
1645
1646
1647
1648
1649
1650
1651
1652
1653
1654
1655
1656
1657
1658
1659
1660
1661
1662
1663
1664
1665
1666
1667
1668
1669
1670
1671
1672
1673
1674
1675
1676
1677
1678
1679
1680
1681
1682
1683
1684
1685
1686
1687
1688
1689
1690
1691
1692
1693
1694
1695
1696
1697
1698
1699
1699
1700
1701
1702
1703
1704
1705
1706
1707
1708
1709
1710
1711
1712
1713
1714
1715
1716
1717
1718
1719
1719
1720
1721
1722
1723
1724
1725
1726
1727
1728
1729
1729
1730
1731
1732
1733
1734
1735
1736
1737
1738
1739
1739
1740
1741
1742
1743
1744
1745
1746
1747
1748
1749
1749
1750
1751
1752
1753
1754
1755
1756
1757
1758
1759
1759
1760
1761
1762
1763
1764
1765
1766
1767
1768
1769
1769
1770
1771
1772
1773
1774
1775
1776
1777
1778
1779
1779
1780
1781
1782
1783
1784
1785
1786
1787
1788
1789
1789
1790
1791
1792
1793
1794
1795
1796
1797
1798
1799
1799
1800
1801
1802
1803
1804
1805
1806
1807
1808
1809
1809
1810
1811
1812
1813
1814
1815
1816
1817
1818
1819
1819
1820
1821
1822
1823
1824
1825
1826
1827
1828
1829
1829
1830
1831
1832
1833
1834
1835
1836
1837
1838
1839
1839
1840
1841
1842
1843
1844
1845
1846
1847
1848
1849
1849
1850
1851
1852
1853
1854
1855
1856
1857
1858
1859
1859
1860
1861
1862
1863
1864
1865
1866
1867
1868
1869
1869
1870
1871
1872
1873
1874
1875
1876
1877
1878
1879
1879
1880
1881
1882
1883
1884
1885
1886
1887
1888
1889
1889
1890
1891
1892
1893
1894
1895
1896
1897
1898
1899
1899
1900
1901
1902
1903
1904
1905
1906
1907
1908
1909
1909
1910
1911
1912
1913
1914
1915
1916
1917
1918
1919
1919
1920
1921
1922
1923
1924
1925
1926
1927
1928
1929
1929
1930
1931
1932
1933
1934
1935
1936
1937
1938
1939
1939
1940
1941
1942
1943
1944
1945
1946
1947
1948
1949
1949
1950
1951
1952
1953
1954
1955
1956
1957
1958
1959
1959
1960
1961
1962
1963
1964
1965
1966
1967
1968
1969
1969
1970
1971
1972
1973
1974
1975
1976
1977
1978
1979
1979
1980
1981
1982
1983
1984
1985
1986
1987
1988
1989
1989
1990
1991
1992
1993
1994
1995
1996
1997
1998
1999
1999
2000
2001
2002
2003
2004
2005
2006
2007
2008
2009
2009
2010
2011
2012
2013
2014
2015
2016
2017
2018
2019
2019
2020
2021
2022
2023
2024
2025
2026
2027
2028
2029
2029
2030
2031
2032
2033
2034
2035
2036
2037
2038
2039
2039
2040
2041
2042
2043
2044
2045
2046
2047
2048
2049
2049
2050
2051
2052
2053
2054
2055
2056
2057
2058
2059
2059
2060
2061
2062
2063
2064
2065
2066
2067
2068
2069
2069
2070
2071
2072
2073
2074
2075
2076
2077
2078
2079
2079
2080
2081
2082
2083
2084
2085
2086
2087
2088
2089
2089
2090
2091
2092
2093
2094
2095
2096
2097
2098
2099
2099
2100
2101
2102
2103
2104
2105
2106
2107
2108
2109
2109
2110
2111
2112
2113
2114
2115
2116
2117
2118
2119
2119
2120
2121
2122
2123
2124
2125
2126
2127
2128
2129
2129
2130
2131
2132
2133
2134
2135
2136
2137
2138
2139
2139
2140
2141
2142
2143
2144
2145
2146
2147
2148
2149
2149
2150
2151
2152
2153
2154
2155
2156
2157
2158
2159
2159
2160
2161
2162
2163
2164
2165
2166
2167
2168
2169
2169
2170
2171
2172
2173
2174
2175
2176
2177
2178
2179
2179
2180
2181
2182
2183
2184
2185
2186
2187
2188
2189
2189
2190
2191
2192
2193
2194
2195
2196
2197
2198
2199
2199
2200
2201
2202
2203
2204
2205
2206
2207
2208
2209
2209
2210
2211
2212
2213
2214
2215
2216
2217
2218
2219
2219
2220
2221
2222
2223
2224
2225
2226
2227
2228
2229
2229
2230
2231
2232
2233
2234
2235
2236
2237
2238
2239
2239
2240
2241
2242
2243
2244
2245
2246
2247
2248
2249
2249
2250
2251
2252
2253
2254
2255
2256
2257
2258
2259
2259
2260
2261
2262
2263
2264
2265
2266
2267
2268
2269
2269
2270
2271
2272
2273
2274
2275
2276
2277
2278
2279
2279
2280
2281
2282
2283
2284
2285
2286
2287
2288
2289
2289
2290
2291
2292
2293
2294
2295
2296
2297
2298
2298
2299
2299
2300
2301
2302
2303
2304
2305
2306
2307
2308
2309
2309
2310
2311
2312
2313
2314
2315
2316
2317
2318
2319
2319
2320
2321
2322
2323
2324
2325
2326
2327
2328
2329
2329
2330
2331
2332
2333
2334
2335
2336
2337
2338
2339
2339
2340
2341
2342
2343
2344
2345
2346
2347
2348
2349
2349
2350
2351
2352
2353
2354
2355
2356
2357
2358
2359
2359
2360
2361
2362
2363
2364
2365
2366
2367
2368
2369
2369
2370
2371
2372
2373
2374
2375
2376
2377
2378
2379
2379
2380
2381
2382
2383
2384
2385
2386
2387
2388
2389
2389
2390
2391
2392
2393
2394
2395
2396
2397
2398
2398
2399
2399
2400
2401
2402
2403
2404
2405
2406
2407
2408
2409
2409
2410
2411
2412
2413
2414
2415
2416
2417
2418
2419
2419
2420
2421
2422
2423
2424
2425
2426
2427
2428
2429
2429
2430
2431
2432
2433
2434
2435
2436
2437
2438
2439
2439
2440
2441
2442
2443
2444
2445
2446
2447
2448
2449
2449
2450
2451
2452
2453
2454
2455
2456
2457
2458
2459
2459
2460
2461
2462
2463
2464
2465
2466
2467
2468
2469
2469
2470
2471
2472
2473
2474
2475
2476
2477
2478
2479
2479
2480
2481
2482
2483
2484
2485
2486
2487
2488
2489
2489
2490
2491
2492
2493
2494
2495
2496
2497
2498
2498
2499
2499
2500
2501
2502
2503
2504
2505
2506
2507
2508
2509
2509
2510
2511
2512
2513
2514
2515
2516
2517
2518
2519
2519
2520
2521
2522
2523
2524
2525
2526
2527
2528
2529
2529
2530
2531
2532
2533
2534
2535
2536
2537
2538
2539
2539
2540
2541
2542
2543
2544
2545
2546
2547
2548
2549
2549
2550
2551
2552
2553
2554
2555
2556
2557
2558
2559
2559
2560
2561
2562
2563
2564
2565
2566
2567
2568
2569
2569
2570
2571
2572
2573
2574
2575
2576
2577
2578
2579
2579
2580
2581
2582
2583
2584
2585
2586
2587
2588
2589
2589
2590
2591
2592
2593
2594
2595
2596
2597
2598
2598
2599
2599
2600
2601
2602
2603
2604
2605
2606
2607
2608
2609
2609
2610
2611
2612
2613
2614
2615
2616
2617
2618
2619
2619
2620
2621
2622
2623
2624
2625
2626
2627
2628
2629
2629
2630
2631
2632
2633
2634
2635
2636
2637
2638
2639
2639
2640
2641
2642
2643
2644
2645
2646
2647
2648
2649
2649
2650
2651
2652
2653
2654
2655
2656
2657
2658
2659
2659
2660
2661
2662
2663
2664
2665
2666
2667
2668
2669
2669
2670
2671
2672
2673
2674
2675
2676
2677
2678
2679
2679
2680
2681
2682
2683
2684
2685
2686
2687
2688
2689
2689
2690
2691
2692
2693
2694
2695
2696
2697
2698
2698
2699
2699
2700
2701
2702
2703
2704
2705
2706
2707
2708
2709
2709
2710
2711
2712
2713
2714
2715
2716
2717
2718
2719
2719
2720
2721
2722
2723
2724
2725
2726
2727
2728
2729
2729
2730
2731
2732
2733
2734
2735
2736
2737
2738
2739
2739
2740
2741
2742
2743
2744
2745
2746
2747
2748
2749
2749
2750
2751
2752
2753
2754
2755
2756
2757
2758
2759
2759
2760
2761
2762
2763
2764
2765
2766
2767
2768
2769
2769
2770
2771
2772
2773
2774
2775
2776
2777
2778
2779
2779
2780
2781
2782
2783
2784
2785
2786
2787
2788
2789
2789
2790
2791
2792
2793
2794
2795
2796
2797
2798
2798
2799
2799
2800
2801
2802
2803
2804
2805
2806
2807
2808
2809
2809
2810
2811
2812
2813
2814
2815
2816
2817
2818
2819
2819
2820
2821
2822
2823
2824
2825
2826
2827
2828
2829
2829
2830
2831
2832
2833
2834
2835
2836
2837
2838
2839
2839
2840
2841
2842
2843
2844
2845
2846
2847
2848
2849
2849
2850
2851
2852
2853
2854
2855
2856
2857
2858
2859
2859
2860
2861
2862
2863
2864
2865
2866
2867
2868
2869
2869
2870
2871
2872
2873
2874
2875
2876
2877
2878
2879
2879
2880
2881
2882
2883
2884
2885
2886
2887
2888
2889
2889
2890
2891
2892
2893
2894
2895
2896
2897
2898
2898
2899
2899
2900
2901
2902
2903
2904
2905
2906
2907
2908
2909
2909
2910
2911
2912
2913
2914
2915
2916
2917
2918
2919
2919
2920
2921
2922
2923
2924
2925
2926
2927
2928
2929
2929
2930
2931
2932
2933
2934
2935
2936
2937
2938
2939
2939
2940
2941
2942
2943
2944
2945
2946
2947
2948
2949
2949
2950
2951
2952
2953
2954
2955
2956
2957
2958
2959
2959
2960
2961
2962
2963
2964
2965
2966
2967
2968
2969
2969
2970
2971
2972
2973
2974
2975
2976
2977
2978
2979
2979
2980
2981
2982
2983
2984
2985
2986
2987
2988
2989
2989
2990
2991
2992
2993
2994
2995
2996
2997
2998
2998
2999
2999
3000
3001
3002
3003
3004
3005
3006
3007
3008
3009
3009
3010
3011
3012
3013
3014
3015
3016
3017
3018
3019
3019
3020
3021
3022
3023
3024
3025
3026
3027
3028
3029
3029
3030
3031
3032
3033
3034
3035
3036
3037
3038
3039
3039
3040
3041
3042
3043
3044
3045
3046
3047
3048
3049
3049
3050
3051
3052
3053
3054
3055
3056
3057
3058
3059
3059
3060
3061
3062
3063
3064
3065
3066
3067
3068
3069
3069
3070
3071
3072
3073
3074
3075
3076
3077
3078
3079
3079
3080
3081
3082
3083
3084
3085
3086
3087
3088
3089
3089
3090
3091
3092
3093
3094
3095
3096
3097
3098
3098
3099
3099
3100
3101
3102
3103
3104
3105
3106
3107
3108
3109
3109
3110
3111
3112
3113
3114
3115
3116
3117
3118
3119
3119
3120
3121
3122
3123
3124
3125
3126
3127
3128
3129
3129
3130
3131
3132
3133
3134
3135
3136
3137
3138
3139
3139
3140
3141
3142
31
```

1188
 1189 necessary. (5) Math is correct; apply requested rounding/units. (6)
 1190 Tone met; no forbidden items. If constraints conflict, prioritize:
 1191 order/sequence > verbatim/ending > forbidden items > numeric/format
 1192 limits (incl. sentence and capitalized-word counts) > keywords/tone >
 1193 any extras. Fix issues and re-check. Remove trailing spaces/newlines
 1194 .",
 1195
 1196
 1197

generate_response_module, Qwen3-8B (acc=44.22)

1200 Read the prompt and list constraints: sequence (repeat verbatim first
 1201 ; nothing before; required exact ending), scope of counts (entire
 1202 response vs answer only), exact phrases/keywords (case/order),
 1203 forbidden items, numeric limits (exact/min sentences, words,
 1204 characters; occurrences; number/format of bullets/items; count of
 1205 capitalized words), tone, and any math/logic with units/rounding.
 1206 Plan the structure accordingly. If required to repeat the request
 1207 verbatim at the beginning, copy it exactly and place it first with
 1208 nothing before; do not add quotes; then proceed to the answer (use a
 1209 single newline as a separator only if not forbidden). Scope all
 1210 counts as specified; if unspecified, apply them to the entire
 1211 response. Meet numeric limits exactly: control sentence count with
 1212 simple sentences and standard punctuation; avoid abbreviations/
 1213 ellipses/parentheticals; deliberately include the needed number of
 1214 Capitalized words and count them. Include required keywords/phrases
 1215 in the stated order/case; exclude forbidden items. Do computations
 1216 accurately; follow rounding/units. If a specific ending is required,
 1217 ensure your final characters are exactly that phrase. Provide step-by
 1218 -step explanation only if explicitly requested; otherwise be concise.
 1219 Before finalizing, recount/recheck against the constraint list and
 1220 adjust. Remove trailing whitespace.
 1221
 1222

generate_response_module, GPT-4.1-mini (acc=54.59)

1223 Pre-check for compliance and correctness: 1) Parse the task into a
 1224 compact internal spec: goal and success criteria; exact required
 1225 outputs; structure (counts/order/labels/delimiters); required first/
 1226 last tokens; exact literals to reproduce and their placement (preserve
 1227 casing/spacing/punctuation); content rules (required/
 1228 forbidden items and exact occurrence/length limits); language/
 1229 modality; numeric rules (use only provided data; units/conversions;
 1230 round only at the end); safety/policy limits. 2) Apply instruction
 1231 hierarchy (system > developer > user); resolve by specificity and
 1232 recency. If full compliance is impossible or unsafe, produce the
 1233 smallest safe compliant output; do not invent facts. 3) Numbers:
 1234 extract data and units, normalize units, compute precisely, verify
 1235 totals/consistency, delay rounding. 4) Verbatim/echo: copy literals
 1236 exactly, respect stated inclusion/exclusion boundaries, no
 1237 normalization or padding before/after echoed segments. 5) Final audit
 1238 : confirm structure and counts, required positions and boundary
 1239 tokens, verbatim exactness, occurrence/length limits, absence of
 1240 forbidden items, language/modality lock, numeric units and rounding,
 1241 safety compliance, and no extra text.

```

1242 ensure_correct_response_module, GPT-4.1-mini (acc=54.59)
1243
1244
1245 Plan then write: decide the exact output shape from the spec (
1246 sections/items/order/labels/delimiters) and fix boundary tokens and
1247 literal placements. Lock the requested language and modality. Use
1248 only provided data for any calculations; normalize units; apply
1249 rounding at the end. Draft the smallest content that satisfies all
1250 constraints; enforce required/forbidden items and exact occurrence/
1251 length counts while writing. Self-check and repair: recount structure
1252 and counts; verify first/last tokens and required positions; ensure
1253 verbatim correctness with no added/omitted characters or padding;
1254 confirm numeric correctness and units; ensure safety/policy
1255 compliance. Output only the final compliant answer.
1256
1257
1258
1259
1260
1261
1262
1263
1264
1265
1266
1267
1268
1269
1270
1271
1272
1273
1274
1275
1276
1277
1278
1279
1280
1281
1282
1283
1284
1285
1286
1287
1288
1289
1290
1291
1292
1293
1294
1295

```